

A Snapshot of Microfluidics in Point-of-Care Diagnostics: Multifaceted Integrity with Materials and Sensors

Garbis Atam Akceoglu, Yeşeren Saylan, and Fatih Inci*

Over four decades, point-of-care (POC) technologies and their pivotal applications in the biomedical arena have increased irrepressibly and allowed to realize the potential of portable and accurate diagnostic strategies. Today, in the light of these advances, POC systems dominate the medical inventions and bring the diagnostics to the bedside settings, potentially minimizing the workload in the centralized laboratories, as well as remarkably reducing the associated-cost and time. In contrast to the conventional technologies, microfluidics paves the way to create more efficient and applicable POC diagnostic devices through their inherent fashions such as minute volume of samples, easy manipulations, shorter assay time, and low-cost production. In this review, the current status and advancements of microfluidic systems along with the current limitations in the aspect of POC diagnostic strategies are elaborated. Further, the integration of novel materials and innovative sensing platforms to the microfluidic systems are comprehensively evaluated to address the real-world challenges for diagnosing various maladies at the POC settings.

1. Introduction

Point-of-care (POC) tests were first used in our lives in the 1960s through the use of strip tests, rapidly measuring blood glucose levels, and later in the late 1970s, personal diagnosis became extremely popular among people with the use of similar strategy in pregnancy tests. Over the next 40 years, advances in the engineering have increased POC applications not only in clinical diagnostics, but also in food safety, environmental monitoring, pharmaceutical industry, military applications, and biosensing realm.^[1–3] All these examples are only snapshots of POC tests reliant on multidisciplinary

devices, where engineering, biochemistry, molecular biology, and biomedical technologies are integrated seamlessly with each other. POC devices have great advantages due to their portability, size, accuracy, and low volume of samples. These advantages are fundamentally changing the workflow of health care systems by shortening the turnaround time, accelerating the clinical decision-making with early treatment possibilities, and enabling to test individuals at resource-scarce settings, including but not limited to disaster areas, remote settings, or physician office with the limited laboratory access. Ultimately, this crucial direction makes health delivery closer to the patient rather than the provider.^[4] In addition, even if the patient is not living in the countryside, the utilization of POC devices at hospitals has exhibited


a remarkable reduction in the duration of hospital stay due to the elimination of time-consuming, centralized laboratory testing.^[5,6] Since the size and portability are great advantages of POC devices, storage, proper usage, and quality control of tests are still unmet challenges. For instance, external factors, e.g., light, humidity, and temperature, hinder the performance of these tests potentially, and thereby, they need to be controlled comprehensively through regular calibrations, technical service, and maintenance performed by trained and experienced personnel, which potentially increase their cost and complexity, as well as limit their utility at the resource-constrained settings.^[7,8]

Microfluidics, on the other hand, denotes a unique opportunity by controlling and manipulating the low volume of liquids (10^{-9} to 10^{-18} L) precisely; handling samples easily; offering inexpensive and large-scale production with the desired parameters; modulating surface properties and integrating multiple control units; and presenting versatile integrity with different sensing modalities. All these features highlight the potential of microfluidics as a full or integrative unit of POC diagnostic devices. From the production perspective, there are many microfabrication methods, such as replica molding, nanoimprint lithography, SU-8 photoresist, rapid prototyping, microinjection molding, and plasma processing.^[9,10] In these platforms, liquids can be controlled in microscale membranes, valves, chambers, reservoirs by mixing or reacting them with each other. Moreover, all these kinds of fashions manipulating the low volume of liquids are creating great opportunities for POC applications, where integration, miniaturization, computerization

Dr. G. A. Akceoglu, Dr. F. Inci
UNAM, National Nanotechnology Research Center
Bilkent University
Ankara 06800, Turkey
E-mail: finci@bilkent.edu.tr

Dr. Y. Saylan
Department of Chemistry
Hacettepe University
Ankara 06800, Turkey

Dr. F. Inci
Institute of Materials Science and Nanotechnology
Bilkent University
Ankara 06800, Turkey

 The ORCID identification number(s) for the author(s) of this article can be found under <https://doi.org/10.1002/admt.202100049>.

DOI: 10.1002/admt.202100049

consistency, and ease-of-use are highly desired.^[11–15] Furthermore, these specific characteristics provide spatiotemporal control of molecules for leveraging the platforms manageability and reducing their size for biomedical applications.^[16–18]

In the recent literature, we are witnesses of the advances in microfluidic fabrication methods, platform integration, and material integration systems that lead to many new microfluidic-integrated POC devices with various functionalities, and consequently, every year the published reports are increasing swiftly and continuously.^[19] In addition, there is a critical need to cover all these aspects by considering the big picture on the implementation and utility of microfluidic systems at the POC settings, as well as their unprecedented integration with materials and sensor systems. Besides these advances, there are remaining challenges, which are majorly related to material type and processing, as well as biocompatibility and toxicity-type issues. In this review, we project to bring all these points to the table, and here, we first emphasize that material integration to the microfluidic platforms leverages the performance of fluidic flow and presents new features such as stability (chemical and/or mechanical), biocompatibility, conductivity (electrical and/or thermal), high aspect ratio, resistivity (acid and/or base), and solvent absorptions (hydrophobicity and/or hydrophilicity). We later continue with versatility of microfluidic platforms for the integration with various sensing modalities, and denote recent POC diagnostic applications to detect rare number of biomarkers, such as proteins, antibodies, small molecules, nucleic acids, as well as whole-cells from clinically relevant fluids. Finally, we overview the strengths and limitations of microfluidic systems and provide potential solutions to hurdle these drawbacks.

2. Material Integration

Microfluidics creates a paramount opportunity to study the behavior of fluids between the range of 10^{-9} to 10^{-18} L through channels at microscales and enables microminimize devices containing chambers and tunnels within the scales of tens to hundreds of micrometers.^[11,19–21] The microfluidic systems have been popularized since the beginning of the 90s^[22,23] for chemical separation applications initially, and in the following years through technological advancements, these systems have been applied to distinct research fields, ranging from synthesis^[24,25] to genomics.^[26] These technological developments are often integrated with “lab-on-a-chip” systems, which can perform accurate processes faster, cheaper, and more portable with minute sample volumes compared to the conventional counterparts.^[27]

On the other hand, in microfluidics systems, choosing the right material is one of the most crucial steps, not only for stability and sensitivity and also for the function of the system. In the last few years, various materials have been assessed to integrate with microfluidics; some of them are successful for specific applications; and some of them are still at the developmental stage.^[28,29] In general, elastomers, thermosets, thermoplastics, silica, glass, paper, carbon nanotube (CNT), graphene-based, hydrogel-based, and inorganic materials are used as a substrate in these systems. Mostly, manufacturing methods for these materials can be i) soft and hard lithographical methods, ii) thermomolding, iii) high- and low-temperature process, and iv) thermal and chemical exfo-

liation. In particular, for the biosensing platforms at the POC settings, a well-aligned and precise combination of both materials and biomolecules is the key to achieve an efficient detection due to the issues on biocompatibility and variable viscosity of biospecimens. In the following sections, we will comprehensively elaborate on all these materials and their integration with microfluidic systems, and provide a detailed comparison list in **Table 1**.

2.1. Polymeric Materials

2.1.1. Elastomer

Elastomers provide a unique structural capability to reshape their molecular conformity under external forces such as stretching or compressing. This reshaping condition is temporary, and it can easily return its original shape without any physical tears or breaks due to its high number of crosslinked bonds in the structure. Basically, the pre-polymers of elastomer are thermally cured at temperatures between $40\text{ }^{\circ}\text{C}$ and $70\text{ }^{\circ}\text{C}$, and they can be cast using photoresist templates at the resolution of nanometer-scales.^[30] Among other polymeric materials, elastomers hold a notable impact in terms of low-cost production, ease-of-microfabrication, and high resistance under various harsh conditions.^[30] As an example, polydimethylsiloxane (PDMS) is well-known and characterized elastomer in microfabrication processes and applied to multiple biological applications.^[31,32] To create functional microfabricated platforms, the soft-lithography method is widely used to combine two or more PDMS layers, constructing multiple units, such as interconnected reservoirs, integrated valves, and enclosed microchannels. Through PDMS valves, a high level of complexity and control of fluidic transportation is enabled for high-throughput applications, such as single-cell analysis, genetics, and sensor systems.^[31,33,34] At the molecular level, PDMS consists of a Si–O backbone structure, creating a porous matrix that provides gas permeability and material transport, as well as it is mostly utilized in biological applications at cell cultures, cell screening, or biochemical assays due to their biocompatibility property.^[35] However, nonspecific and noncontrollable molecule absorption at channel walls, liquid evaporation, and subsequent gradient formation through evaporation and internal flow hinder its broad applicability and utility for biological applications.^[36–38] Another limitation of PDMS material is its channel deformation and acid/base resistivity problems.^[29,39] While there are limiting factors, it is obvious that PDMS is still one of the most utilized materials in microfluidic devices, where cellular entities are integrated.^[40,41] Recent studies support our perspective, and nowadays, PDMS has been utilized to develop flexible electronics, impacting the innovation of bendable, wearable, and stretchable electronics, including smart bandages, which are integrated with biosensors to monitor health status.^[42–44]

2.1.2. Thermosets

Thermosets are mostly used in negative photoresist applications for the fabrication of microfluidic systems.^[45] In general, heat, light, ultraviolet, and other radiation-related effects form strong crosslinking during the fabrication. This curing

Table 1. Evaluation of material types in terms of fabrication strategy, functionality, and limitations.

Material type	Fabrication strategy	Transducer	Valve	Channel	Limitations	Ref.
Elastomer	<ul style="list-style-type: none"> Stretching Compressing Soft lithography 	–	✓	✓	<ul style="list-style-type: none"> Nonspecific and noncontrollable molecule absorption Liquid evaporation and acid/base resistivity issues 	[29–31,33,34,36–39]
Thermosets	<ul style="list-style-type: none"> Radiation-related strategies 	–	✓	–	<ul style="list-style-type: none"> Fabrication cost Brittleness Limited integration 	[46,49]
Thermoplastics	<ul style="list-style-type: none"> Thermomolding 	–	–	✓	<ul style="list-style-type: none"> Expensive Requires metal or silicon templates Limited conformal connection Not easy adaptation to cell-based studies 	[46,58,59]
Hydrogels	<ul style="list-style-type: none"> Physical or chemical crosslinking 	–	–	✓	<ul style="list-style-type: none"> Limited stiffness properties Requires expensive instrumentation Production processes are not scalable easily 	[61,63,316–319]
Silica and glass	<ul style="list-style-type: none"> Microfabrication techniques 	–	✓	✓	<ul style="list-style-type: none"> Expensive and time-consuming fabrication process Highly fragile with low flexibility Challenges in chemical modifications 	[83,90]
Ceramic	<ul style="list-style-type: none"> Firing in a kiln 	–	–	✓	<ul style="list-style-type: none"> Complex sintering behavior Variable thermomechanical properties are needed for each parameter Chemical incompatibility High production cost Unstable shrinkage properties 	[93,94,320]
Paper	<ul style="list-style-type: none"> Lithographic methods Cutting and/or printing methods 	–	–	✓	<ul style="list-style-type: none"> Cellulosic fibers may fill channels to prevent wicking flow Low-throughput and semiquantitative detection 	[109,113,114,120,121]
Carbon nanotubes	<ul style="list-style-type: none"> Electric arc discharge Laser ablation CVD process 	–	–	✓	<ul style="list-style-type: none"> Bio-safety issues Need for harsh chemicals 	[122,138–143]
Graphene	<ul style="list-style-type: none"> Scotch tape method Thermal and chemical exfoliation CVD process 	✓	–	–	<ul style="list-style-type: none"> Use of explosive and toxic chemicals Difficult to dissolve in water and common organic solvents Paucity of methods to obtain graphene materials with appropriate structure and properties 	[145,242,321–324]

process is an irreversible chemical reaction, and it creates a rigid structure that cannot reshape the original structure like elastomers.^[46] After curing, thermosets become optically transparent, structurally strong, and high resistance to high temperatures and chemical solvents. These acquired features make thermosets notable materials for microfluidic tools, especially in optical sensor designs.^[47] In the microfluidic realm, the SU-8 photore-sist material is a well-known thermoset, containing 8 epoxy groups in the structure, and can be easily patterned and coated within a range of nanometer to millimeter scale.^[48–50] In contrary to elastomers, the strong and rigid structure of SU-8, however, causes large internal stress and makes them highly brittle that cannot be integrated with joint parts and units of microfluidic systems such as diaphragm valves. Fabrication cost is also another obstacle for their large-use in microtechnological applications.^[49] Recently, Schmidt et al. fabricated a free-standing and flexible SU-8-based microfluidic sensor, measuring the impedance spectrum of distilled water and ethanol mixture in the concentration range of 2–10% (Figure 1A).^[51] The results of

the complex impedance and phase measurements showed a frequency range of 10 kHz–10 MHz, and this design enabled to create a reduced-scale sensing device, revealing an innovative way of miniaturization for POC applications. Overall, their brittle structure and limited integration with joint parts restrict the integration of thermosets partially with up-to-date systems and applications, such as wearable microfluidics and fully controlled chip-based genomic studies.

2.1.3. Thermoplastics

Thermoplastics belong to the polymers family with many differences compared to elastomers and thermosets. For instance, they can be reshaped after being cured, and even if you reheat and reshape them again multiple times, their chemical and physical stability will remain constant for different pressure and temperature levels. They also provide a soft structure at glass transition temperatures (T_g), enabling them more processable

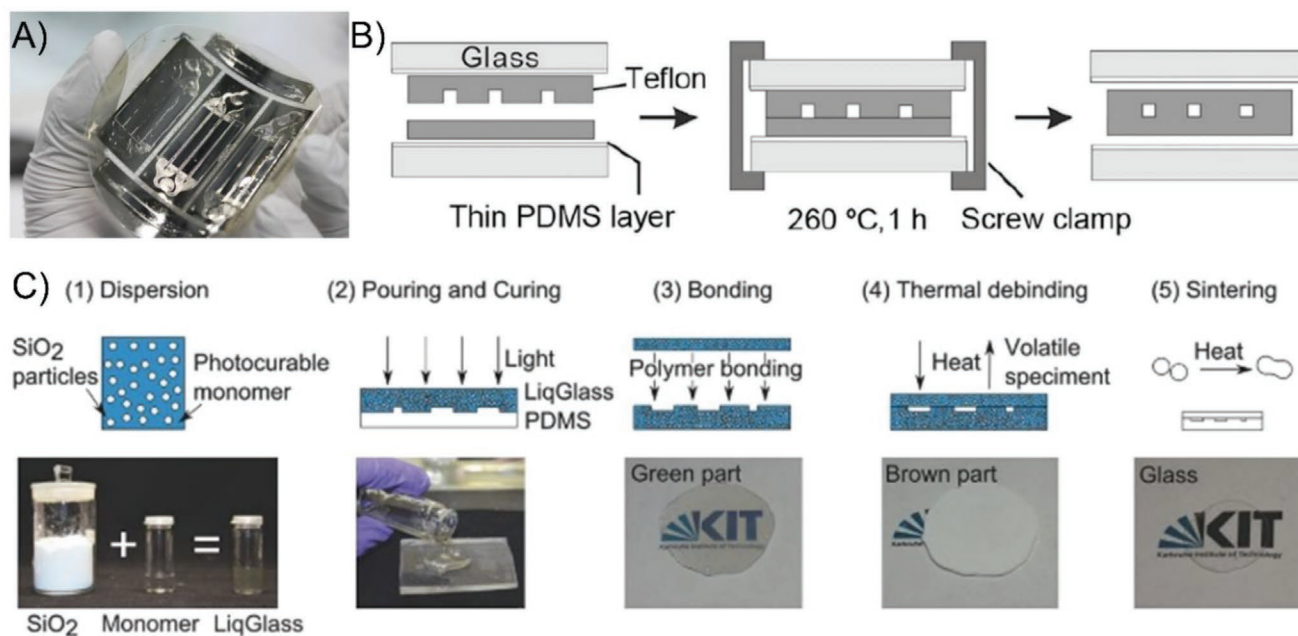


Figure 1. A) A flexible SU-8-stemmed microfluidic sensor for monitoring the impedance spectrum. Reproduced with permission.^[51] Copyright 2016, Copernicus Publications. B) Fabrication steps of Teflon microfluidic device under certain pressure and heat. Reproduced with permission.^[52] Copyright 2011, Proceedings of the National Academy of Sciences of the United States of America. C) Fabrication steps of liquid glass material from photocurable amorphous silica nanocomposite. Reproduced with permission.^[84] Copyright 2016, Wiley-VCH.

for molding and bonding applications. Typical thermoplastics used in microfluidics include polycarbonate (PC), polyethylene terephthalate (PET), polystyrene (PS), polymethyl methacrylate (PMMA), and polyvinylchloride (PVC).^[46]

Thermoplastics are fabricated by the thermomolding method, which provides an opportunity for mass-production (thousands of replicas) at reduced costs, yet it requires templates in metal or silicon for operating at high temperatures. Despite an excellent fashion for mass-production, they are not cost-effective for prototyping.^[46] Although there are some rapid versions of this method for prototyping, they are limited to thermoplastics only. Recently, the current curing process has been updated, thereby it would be applied to all types of thermoplastics.^[37,52] Thermoplastics offer substantially low-cost raw material/manufacturing. Further, they show good mechanical stability, acid/base resistivity, and their water and organic solvent absorptions are very low, making them good biocompatible material for bioanalytic assays.^[53–55] Additionally, applications like oxygen plasma treatments covalently modify thermoplastic surfaces and make them more stable compared to other polymers, such as PDMS. Through these adjustments, they can be integrated easily with electrodes for digital microfluidics.^[56]

Teflon materials are known for their nonstickiness, inertness, and antifouling properties, and they can be turned into microfluidic devices due to their thermally bonding properties (Figure 1B).^[52] Perfluoroalkoxy (TeflonPFA) and fluorinated ethylene propylene (TeflonFEP) are some examples of thermoprocessable microfluidic structures, which show compatibility to high organic solvents, and provide biocompatibility and antifouling properties. Immobilization of biological materials is an essential method for biotechnological applications that are often applied into microfluidics systems to decorate catalytic

and/or analytic microreactors inside microchannels in order to increase efficiency and reduce the associated steps for downstream analyses. For instance, highly dense microarray patterns of *Pseudomonas putida*, *Escherichia coli* (*E. coli*), and *Bacillus subtilis* were immobilized on perfluoroalkoxy materials. Later, another integrated system which is coupled with polystyrene-based microfluidic chip and electrospray ionization mass spectrometry, has denoted on-chip protein digestion and online analysis.^[57] Under a flow rate of 100 nL min⁻¹, 96% of sequence coverage was obtained inside this immobilized enzymatic reactor within 8.4 min. Furthermore, this system was able to detect cytochrome c down to 10 µg mL⁻¹.

Besides all these properties, we consider some drawbacks for thermoplastics used in microfluidics: i) thermoplastics cannot create a conformal connection with other materials, leading to difficulties at sealing their channels. ii) Their rigid structure and limited gas permeability also lead to challenges in cell studies, limiting cellular viability and cell adherence.^[58,59]

2.1.4. Hydrogels

Hydrogels create a 3D network composed of hydrophilic polymers with the properties of swelling in the presence of water, as well as holding water molecules without altering their structure.^[60] Therefore, hydrogels offer many distinct properties than that we mentioned in the earlier sections. Briefly, their most vital feature that distinguishes them from the other polymers is to absorb hundreds of times of water in respect to their own mass and being insoluble in water while maintaining their structure through chemical or physical crosslinking.^[61] They can be classified in two major groups according to their

origins:^[60] i) natural hydrogels include gelatin, collagen, silk, agarose, and so on, whereas ii) synthetic polymers are, for instance, poly(ethylene glycol) (PEG), poly(vinyl alcohol) (PVA), poly(*n*-iso-propylacrilamide) (pNIPAAm), and poly(hydroxyethyl methacrylate) (pHEMA). In addition, once the 3D of their skeleton structure is formed after the polymerization reaction, they can be utilized in many purposes, including cancer therapy, drug delivery, sensors, tissue engineering, and adhesive research.^[60,62–64] In hydrogel-based microfluidic systems, recognition elements are typically confined inside hydrogels, which are encircled by microchannels, creating a sample flow. This harmonious operation of hydrogels and microfluidic systems enables the analysis of many different products, and ultimately, they denote new platforms to maximize their individual advantages. In addition, hydrogels have other features that make them indispensable, including i) biocompatibility,^[65–68] ii) ease-of-modification according to the physical size of biomolecules to be analyzed; iii) responding against external stimuli, such as temperature, pH, light and electrical stimulus;^[60,69] iv) structurally and mechanically resembling extracellular matrix;^[70] and v) protecting the biological entities in a 3D network while creating them in a hydrated environment, which mimics their physiological condition.^[70–73] Hence, while preventing the degradation and nonspecific adsorption of these biological entities, hydrogels minimize their denaturation and enable to perform their biological functions for a longer time.^[72,74–76] Through utilization of these features, different microfluidic systems have been established, and for instance, Powers et al. and Lee et al. were able to measure the kinase activity in the cells by confining the phosphorylation substrate inside the hydrogel structure.^[77,78] This study also examines how cancer cells react to kinase inhibitors and enable personalized therapy eventually. As another example, Piao et al. developed a microfluidic system for sensing glucose by embedding glucose oxidase (GOx) in poly(ethylene glycol) diacrylate (PEG-DA) synthetic hydrogels.^[79] In this system, they were able to determine glucose concentrations by the means of fluorescence signals through the production of droplets, where fluorescent intensities were linearly proportional to glucose concentration up to 3×10^{-3} M with a detection limit of 10×10^{-6} M. Another study was reported by Puchberger et al., who modified PEG-DA hydrogels in order to recognize MMP-9.^[74] This system determines the enzyme activity by cleaving collagen substrates, and it consequently measures the intensity of green fluorescence light. As a result, the sensitivity of this device was leveraged by longer incubation time, and it was able to detect $10 \mu\text{g mL}^{-1}$ of analytes within 15 min. Hence, they have depicted the cell counting and colorimetric protein recognition in the same system. Apart from recognizing bioassays, these systems would be used to perform separation for the micro-sized structures. In this way, continuous operation, small size, shorter analysis time, and low sample amount can be listed as their advantages. For example, in some reports,^[80–82] we witness their successful operations for capturing and isolating blood cells when unprocessed blood samples were applied directly into these systems without the need for any incubation or centrifugation processes. Our perspective on hydrogels and their integration with microfluidic systems is that this mutual interaction is at the beginning, but there are multiple opportunities as the “low-hanging fruit” in the field;

for instance, the directed self-assembly of hydrogels on-chip systems, artificial tissue or organ construction in microfluidic channels, and 3D printing of specialized hydrogels and microfluidic production in real-time can be listed, but not limited to these examples.

2.2. Inorganic Materials

2.2.1. Silica and Glass

Silica and glass are the first materials to fabricate capillaries and microchannels due to their ease-of-mass production, high availability, and their facile microfabrication techniques.^[83] Typically, they processed with standard photolithography methods, applying a thin layer of photoresist to a wafer surface, and afterward, exposing an ultraviolet light to transfer the micro patterns/motifs onto a transparency mask.^[84] In particular, glass holds multiple advantages since it is reusable, biocompatible, well-hydrophilic, optically transparent with lower fluorescence background, and stable surface properties (e.g., wettability, surface adsorption, and surface reactivity), as well as it provides strong anodic bonding capability that allows great resistance under high pressures.^[85–89] Despite these vital capabilities of glass utilized in microfluidic platforms, today glass is not the superior material because it requires expensive and time-consuming fabrication processes, and also, it is highly fragile with low flexibility.^[90] There are a few examples of glass-based microfluidic platforms such as label-free immune detection systems by creating various PC channels with different colloidal spheres to detect human IgG protein^[91] or volumetric bar-chart chips based on slip chip technologies, which requires only a facile fabrication method, and it does not require any bonding steps or pumps or valves, denoting very suitable material for resource-scarce settings.^[92] Recently, a liquid form of glass was produced through a photo-curable amorphous silica nanocomposite (Figure 1C), potentially accelerating the prototyping and fabrication of microstructures on-chip platforms, and at the same, reducing the cost and the need for clean-room infrastructure or any hazardous chemicals.^[84]

Despite new fashions introduced to the glass or silica materials, their rigidity and existing difficulties to chemically modify their structures are remaining challenges for microfluidics. On the other hand, clear transparency on glass materials is essential for the applications of optical sensing strategies, and further investigations in making them more flexible and chemically active would open new horizons for this realm.

2.2.2. Ceramic

Low temperature co-fired ceramics (LTCC) are aluminum oxide-based materials with laminate sheet structures. This material provides notable resistance to high temperatures, and it can be produced with complex 3D shapes for packaging of integrated circuits and other systems in package components for a long time.^[93,94] In recent years, LTCC has offered several advantages over the inorganic and polymer materials, and accordingly, it has been applied to the microfluidic research

due to its unique fashions, including cost-effective, facile, and efficient production of numerous layers in 3D complex structures; no need for a clean room facility with the utilization of corrosive and toxic reagents in the production line; chemically inert; and most importantly, good biocompatibility.^[94,95] LTCC thus provides critical aspects over the materials commonly used in microfluidic systems, e.g., glass, silicon and polymers. LTCC-stemmed microfluidic systems have been expanded to a variety of applications, including cell culture analysis, environmental, microreactors for PCR applications, and biosensors.^[96–99] For instance, Vasudev et al. have developed a fully automated microfluidic system based on LTCC and they integrated this system with interdigitated electrodes, functioning as an electrochemical sensor.^[100] To detect cortisol, the electrodes are modified with self-assembled monolayers and embedded in 3D microfluidic channels. The sensor on this system have exhibited a linear range between 36 pg mL⁻¹ and 36 ng mL⁻¹ (10×10^{-12} M– 100×10^{-9} M) and a sensitivity of 0.207 mA M⁻¹. This study demonstrates an inexpensive microfluidic system composed of LTCC as a promising POC system for the detection of biomolecules. In the near future, we foresee the effective and broader use of LTCC-based systems for such applications.

2.3. Paper

For decades, paper-based lateral-flow assay (LFA) has been one of the most employed strategies in the biosensing realm.^[101] After Martinez and co-workers introduced the first paper-based microfluidic system (μ PAD) for chemical analysis, this material has provided more practical applications in the fields of diagnostics and biosensing.^[102–108] Briefly, μ PADs create hydrophobic patterns as barriers on hydrophilic paper substrates to avoid liquid motion, thus serving

as a channel network.^[102,109–112] Fundamentally, these patterns and channel fabrication methods can be classified: i) lithographic methods, including laser treatment, inkjet etching, photolithography, and wet etching; and ii) cutting and printing methods such as wax printing, paper cutting, and shaping, ink stamping, plasma treatment, screen-printing, chemical vapor-phase deposition, inkjet printing, hand-held corona treatment, flexographic printing, plotting, and lacquer spraying (**Figure 2**).^[109,113,114] In the biosensing and biomedical engineering fields, the paper as a substrate has been deployed to an enzyme-linked immunosorbent assay (ELISA) format to detect a variety of proteins,^[102] viral antigens,^[115] eukaryotic cells,^[102] and bacteria.^[116] Further investigations denote that paper-based substrates were also be integrated with light-emitting diodes (LEDs) for fluorescence measurements.^[117] Compared to the other microfluidic supplies, such as glass, silicon, or polymer substrates, paper-based platforms offer flexible, disposable, user-friendly, rapid, low-cost, biocompatible, and robust solutions to the field.^[114,118] Particularly, nitrocellulose and cellulosic fibers in paper structures enable natural capillary function without the need for any external assistance.^[119] However, at the closed channel systems, these fibers fill channels and prevent wicking flow. By fabricating open channels, paper-based microfluidic platforms overcome some of these challenges.^[120,121]

On the other hand, we here remind that low-throughput, semiquantitative detection, and less capability for large sample volumes are still bottlenecks to broaden their applications in the field. In addition, printing strategies are easy manipulation strategies for paper-based platforms, generating channels and constraining assay volume. In the experimental design, the intrinsic roughness of the paper, however, needs to be re-considered for the smooth and efficient flow of fluids, and otherwise, reproducibility of the assay would be hindered.

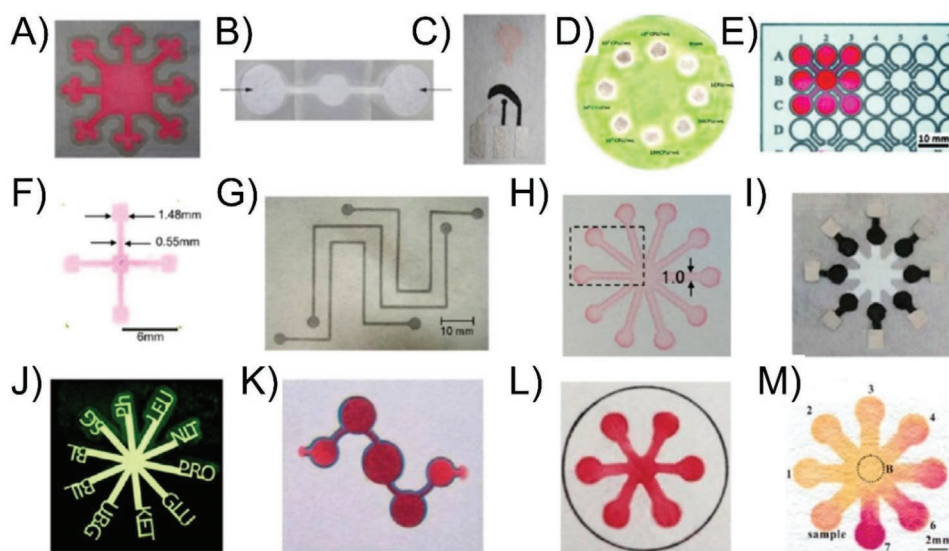


Figure 2. Paper-based microfluidic devices with various fabrication methods. A) Wax stamping and movable type printing, B) wax dipping, C) screen-printed wax device and the demonstration of electrodes, D) a stencil-assisted wax drawing, E) wax printing, F) inkjet etching of polystyrene in paper, G) inkjet printing of alkyl ketene dimer (AKD), H) flexographic printing of polystyrene, I) photoresist patterning via screen-printed electrodes, J) computer-operated knife cutting in nitrocellulose, K) hollow channels using a laser-cut strategy, L) the deposition of vapor-phase polymer, and M) through chemical modifications with alkylsilane self-assembling and UV/O₃ patterning. Reproduced with permission.^[113] Copyright 2015, American Chemical Society.

2.4. Carbonaceous Materials

2.4.1. Carbon Nanotubes (CNTs)

Today, CNTs have been utilized in the fabrication and applications of many modern technological devices because of their ultrasensitivity, inexpensive production, easy functionality, and facile use. Basically, they are produced by high temperature (e.g., electric arc discharge, laser ablation, etc.) and low temperature (CVD) processes.^[122] With the development of microfluidic systems and the need for new materials, CNTs have garnered more attention in this realm, especially owing to their electrical and thermal conductivity, high aspect ratio, chemical and mechanical stability, and superhydrophobicity features. Their superhydrophobic feature enables the great control in analytes that are difficult to dissolve in aqueous solutions for fluid flow by minimizing the contact surface between the channels. Moreover, for instance, if CNTs are designed in patterned arrays of hexagonal pillars at different size, their potential difference between surrounding electrolyte will never exceed the overpotential for electrolysis. This will avoid bubble formation and vastly increase the electrical field strength. This situation is very suitable for electroosmotic pumping of liquids with field strength up to several kV cm^{-1} .^[123–125]

Furthermore, the CNT surfaces can be easily functionalized with multi-label strategies (antibodies,^[126,127] proteins,^[128] aptamers,^[129] enzymes,^[130] polymers, and transition metal hexacyanoferrates.^[131–133] through surface chemistry approaches in order to enable the sensitive detection of biomarkers with the detection limit of 100 amol mL^{-1} (4 pg mL^{-1}) for prostate-specific antigen (PSA) and $25 \times 10^{-15} \text{ M}$ (0.5 pg mL^{-1}) for interleukin-6 calf serum.^[134,135] Due to their selective permeability and hollow structure, CNTs are also engineered to separate undesired substances from microfluidic channels in order to increase specificity, concentrate samples, and also leverage their sensitivity.^[136] For example, Garcia and Sansom evaluated membrane-spanning SWCNTs by using transportation of various ions like calcium, potassium and chloride. This study concluded that the overall selectivity was mostly affected by the net charge of the CNT filters.^[137]

Regarding CNTs, we point out some concerns: i) bio-safety issues limit their utility in wearable sensors and drug monitoring systems,^[138–140] and ii) they also require harsh chemicals to be modified and integrated with biomedical devices.^[141–143] All these arguments create fabrication and application-wise challenges for their integration into microfluidic and sensor systems.

2.4.2. Graphene

Graphene material—2D honeycomb lattice with a single atomic layer, has garnered great attention in the fields of biomedical engineering, biosensing, medical diagnostics, industry, and environmental engineering due to its electronic, thermal, and mechanical features.^[144] Depending on the production techniques, including scotch tape method, thermal and chemical exfoliation or CVD, graphene can be obtained in a pristine or oxidized form. However, unlike pristine graphene, an oxidized

form of graphene (graphene oxide (GO)), is especially preferred since structural defects and functional groups on the GO surface offers an ideal material for electrochemical-based biosensing applications.^[145] Furthermore, it provides versatility to immobilize biological and polymeric probes, such as DNA, proteins, amino cyclodextrin, or betapoly-L-lysine,^[146–149] and also enables the detection of biochemical analytes, e.g., hydrogen peroxide, glucose,^[150] dopamine, and DNA molecules.^[151–153] Besides covalent bonding, hydrophilic and π - π interactions can also be utilized in these systems regardless of altering the intrinsic properties of graphene material.^[154] In addition, graphene denotes good biocompatibility, chemical inertness, and high electrical conductivity, which are key features to create biosensing tools and diagnostic platforms for POC testing.^[155–158]

As an example, screen-printed electrodes (SPE) have been largely utilized in graphene-based POC devices.^[145,159] As another example, Li et al. developed a portable, highly sensitive, disposable, and low-cost sensing transducer platform using a modified film (i.e., nafion-graphene composite film), which was fabricated based on screen-printing of carbon electrodes, and this platform was employed to detect HIV-1.^[160] Recently, a (poly(3,4-ethylenedioxythiophene):poly(styrenesulfonate) (PEDOT:PSS)) and rGO coated paper was developed as a disposable electrochemical sensor in order to detect carcino-embryonic antigens via the target-induced proximity hybridization.^[161] Here, SPE systems were also successfully modified with graphene/polyaniline/Au/glucose oxidase nanobiocomposites and combined with paper-based devices in order to determine glucose levels in whole blood samples.^[162] Besides paper-based devices, graphene materials were also coupled with metal nanoparticles and aptamers for improving the sensitivity and selectivity of biosensors.^[163]

Looking back over the past decade, graphene is still one of the most employed substrates at biosensing platforms, especially in electrochemical sensors, as it provides high stability, sensitivity, and specificity properties when coupled with biomolecules. Among the other fabrication methods, SPE fabrication holds a great impact due to the facile application and low-cost production.^[164–167] Furthermore, graphene integrity with plasmonic and photonic structures provides metamaterials, boosting their optical properties and potentially enhancing their sensitivity and analytical assay performance remarkable.^[168,169] All these features indicate that we are at the beginning of the graphene journey in microfluidics and sensing modalities, and their integration with flexible materials would accelerate and potentially dominate their utility in wearable diagnostics systems in the near future.^[170,171]

3. A Recent Update in Microfluidic Fabrication: 3D Printing

Along with the aforementioned materials, we have introduced the existing fabrication methods, such as replica molding, nanoimprint lithography, SU-8 photoresist, rapid prototyping, microinjection molding, and plasma processing. However, all these conventional methods impede significantly with lengthy production, imprecision, high-cost, and difficulties in design changes.^[172] In addition, the materials used by the conventional

means, have some weaknesses; for instance, PDMS has surface adsorption that increase nonspecific binding in sensor and cell-based applications, and solvent swelling that limits the cellular growth for a long period of time; PMMA or cyclic olefin copolymer has limited gas permeability and high rigidity.^[172] In this regard, the 3D printing strategies have revitalized the current practice in microfluidic fabrication recently.^[173] Through many investigations, some of the challenges associated with microfluidic fabrication have been addressed by the 3D printing platforms and designing tools. Briefly, the 3D printing strategy i) enables rapid and modular design through easy-to-use 3D computer-aided design (CAD) software; ii) allows facile design and rapid prototyping compared to lithographic methods; iii) reduces time to fabricate the devices; iv) decreases the total cost; v) requires less number of steps (basically design, process, and cleaning); vi) eliminates the need for clean-room facilities; vii) facilitates to share the design parameters more conveniently; viii) provides opportunities to select a variety of resins; and ix) presents more flexibility to gain benefits to the base-materials, such as antifouling, biocompatibility, and porosity that are crucial for sensor and cell-based studies.^[172,174]

3.1. 3D Printing-based Fabrication Methods

On the other hand, millifluidics is one of the well-developed areas by the 3D printing strategy.^[175] Here, the structures are implemented in large microfluidic to millifluidic devices, sizing more than 200 μm , and they are fabricated by stereolithography (SLA), fused deposition modelling (FDM) or PolyJet (PJ) 3D printers. The first approach, i.e., SLA, utilizes a UV laser or a different light source to allow polymerization in a photosensitive resin complex. The light source can be either i) a single-point laser illuminating every voxel separately or ii) a digital micromirror-array device (DLP) to enable the curing of the whole layer concurrently.^[176] Layer-by-layer construction of the structures takes the place once the cured resin is accommodated up or down, and the next layer is processed accordingly.^[177] Recent advances have introduced their updated versions, and two-photon polymerization (2PP), for instance, utilizes femtosecond laser pulses to persuade crosslinking of the material, addressing the need for layer-by-layer formation through the nonlinear nature of the process, and it also provides the channel features down to the nanoscale.^[178] Continuous liquid interface printing (CLIP)—a recently developed SLA method, presents high-speed processing and allows to construct structures continuously in z-axis by using an oxygen-permeable membrane on the bottom of the resin vat.^[176,179] Since oxygen prevents the polymerization of the resin, the process forms a dead-zone that limits the printing process from sticking to the vat, and the thickness of dead-zone is reliant on the speed as slower speed results in thicker means. On the other hand, the resolution is mainly limited to the light absorbance of resin as the printing is associated with the penetration depth,^[172,176,179] thereby higher resolution requires more time for proper formation. By altering the incident light intensities, tunable dead-zone regions is formed by this methodology.^[180] CLIP holds great potential to manufacture the means in bulk, yet there is a great need to produce microfluidic-type devices as

the method requires more resolution to achieve such dimensions and to create enclosed features.^[172] Some of these challenges have been solved by illuminating a rotating volume of photosensitive material with a dynamically evolving light pattern, termed as tomographic reconstruction.^[181] This strategy was capable of producing features as small as 300 μm in specialized acrylate polymers; it was able to print soft objects into a gelatin methacrylate (GelMA)-based hydrogels, and also fabricate the objects in centimeter-scale within 30–120 s.

The second method, i.e., FDM, utilizes a heated-nozzle to deposit a molten thermoplastic in a layer-by-layer formation. On the course of the process, the material combines with the earlier layer and becomes cold to form a solid state, thereby multilayers are likely constructed, and diverse materials can be used in the process.^[182] The resolution is often limited to the motor control, reproducibility of filament extrusion, surface striations and roughness. The PJ, the latter strategy, employs inkjet print-heads to jet two materials (i.e., a photosensitive build material and a sacrificial supporting material) to construct layer-by-layer structures.^[176] Once a layer is completed, the first material is cured by an UV exposure, and it is prepared for the next layer until the completion of the entire process and the removal of the sacrificial wax. This strategy hence enables to deposit a multitude of materials within the same run.^[183] Consequently, the FDM and PJ methods share similar obstacles, and they have been explicitly indicated by an earlier review.^[184] In this review, we plan to summarize some of the vital challenges and their potential solutions. i) The feature size could be improved by decreasing the size of nozzles in FDM or the size of droplets produced in PJ, and also, these updates possibly improve the surface roughness. ii) The materials hold critical role in FDM and PJ printing. For instance, flexible and stretchable materials composed of urethane diacrylate along with a linear and semicrystalline polymer were printed, and the device presented shape memory and self-healing fashions.^[185] Further investigations were attempted to benchmark the auto-fluorescence, transparency, biocompatibility, leakage, and the channel dimensions of the produced devices.^[186,187] However, the other challenges come to the table, which are iii) the removal of support material once the completion of the channel formation, and also, iv) commercially available support materials are not optimized for clearing in micrometer dimensions, whereas the removal process is achieved mainly through flushing, sonication, and/or heating processes for many hours.^[172]

3.2. Basic Units in Millifluidics Developed by the 3D Printing

The printing methods are selected according to the dimensions of the structures in millifluidics. Devices developed by one of these methods can include either passively or actively controlled units.^[172] Passive millifluidics, for instance, contains units such as channels, reservoirs, fluid control units, and fluidic mixers that are not integrated with the external sources to stimulate the system. As an example, a new extension of laminar flow patterning was demonstrated using Darcy flow within a 3D hydrogel.^[188] Basically, the researchers developed a three-inlet device filled with collagen, and the concentration profile was fine-tuned by the inlet pressures, enabling the solutions to be

travelled within 50 μm accuracy inside the gel that were further validated with fluorescent polysaccharides. Moreover, they updated the device by including an extra two inlets to control the concentration profile in vertical position, thereby showing an easily extensible method to manage the concentration profile in 3D. In the future, this method would have a vital impact to mimic drug delivery applications on a chip. In a different study, a 3D-printed capillary circuit (3D-CC) platform was developed to analyze blood viscosity through hand-powered device operation.^[189] In the design, there were parallel capillary networks to compare the volumetric flow rates of the control and the test fluid, as well as graduated fluidic chambers to allow naked-eye readout. The device was first characterized with Newtonian fluids (e.g., glycerol and canola oil) spanning from 4.8–71.2 cP of fluid viscosities, and later on, the researchers validated the system with whole blood under controlled shear-rate settings (48.5–482.1 s^{-1}) through a simple operation, such as withdrawing and pushing the plunger of a syringe, presenting a cost-effective and facile method that would be an alternative to the conventional viscometers, and also, being implemented easily to multiple field settings. Moreover, it is worth to highlight that materials used for developing passive millifluidic devices is the most vital parameter, and their surface features, such as roughness, transparency, and sealing, are the key players in the fabrication although the smoothest surfaces are developed by SLA method with the best resolution parameters.

The second regard, i.e., active millifluidics, requires external sources to stimulate the system, containing active valve and pump units. The valves in active millifluidics have different configurations; for instance, deflected membranes for driving the fluid flow,^[190] rotating valve system,^[191] and the ones powered by an evaporating liquid vapor pressure.^[192] All these valve means are actively integrated with external pressure or pump systems, and their size are mostly within the range of >1 mm, leading to notable dead-volume. The droplet generators are the other important active features, and they are benchmarked through the output parameters, such as the size, homogeneity, and layer features of droplets.^[193,194] Droplet generation on microfluidics have garnered great interest in cell-focused researches, such as cell encapsulation,^[195] organ-mimicking structures,^[196] amplification of genetic materials,^[197] drug delivery/release assays,^[198–200] and so on. For instance, a 3D printed device was developed to produce sub-millimetric hollow hydrogel spheres, encapsulating cells and mimicking extracellular matrix (ECM) with a few micrometers of thickness.^[201] Alginate hydrogel-stemmed spherical capsules were produced through multilayered jet, which was generated through co-extrusion of a coaxial flow device. In these capsules, human neural stem cells (hNSC) derived from human induced pluripotent stem cells (hiPSC) were encapsulated, and the inner walls of the capsules were decorated with a continuous ECM layer that was tethered to the hydrogels to imitate the basal membrane of the cellular niche. Due to the sufficient mimicking capacity of the capsules, hNSCs were further differentiated into neurons with appropriate cell viability. Consequently, this study demonstrated how 3D printed device could form cell encapsulating hydrogels with multilayers of continuous ECM-type materials, as well as it provided a notable potential to broaden the field of cell encapsulation technology with more sizable and batch manufacturing process.

Since the limited number of support materials are allowed to use in the commercial printers, and the customized materials can break their warranties as expressed by the companies, the advancements in new materials production is limited to the research settings mostly. Given the low demand in new material use as the manufacturers have pointed out, there is a self-defeating cycle for developing new supports or resins. Such attempts would improve the current status and the removal of support material or resins could be performed through different mechanisms reliant on solubility, melting, or viscosity.

Overall, 3D printing of microfluidic devices has revolutionized the field by introducing more rapid and inexpensive fashions, and at the same time, keeping the potential for bulk production with repeatable structures, thereby it also paves the way for the commercialization of these devices. Considering that PDMS and soft lithography techniques has taken more than two decades, which the 3D printing has already been there for a short period of time and served as their succession. Advances in manufacturing and nanotechnology revolution have accelerated the 3D printing strategies in terms of instrumentation and material types as the earlier microfluidic strategies have not seen before. With rapid updates in this strategy, we anticipate that the 3D printing strategy would take the lead in the microfluidic realm, yet some points need to be re-visited on the course of the development. First, the expansion of material types and their facile processes would be crucial in rapid deployment of this strategy to not only microfluidics, and also many different fields. There have been significant efforts, and some of them were stated above, however these methods need to be simplified for the researchers, and ultimately for the end-users in prototyping and manufacturing stages. Second, more accurate dissemination of the instrument would help producing the microfluidic devices with the advertised resolution rates. Third, more efforts would be needed for appropriate material processing during the application. For instance, in the analytical applications, the apparent impediment of 3D printed microfluidics is the low transparency,^[202,203] minimizing their utility in the integration of optical sensors. Recent advances have tackled this issue through alterations in printing orientation,^[174] achieving sufficient transparency (transmittance $\approx 80\%$). Such improvements in the protocols would be standardized, and maybe, the default parameters would be integrated with the software, hence enabling easy adaptation. Fourth, the expansion of different materials to all 3D printing instrument would increase the standardization of the technique. Therefore, sharing the design parameters would be only step for bulk production at different sites. In addition, increasing the versatility of CAD-stemmed software would have significant role at this step. Currently, we are at the stage of characterization and material adaptation to this strategy, and we expect that for less than a decade, the 3D printing would be dominant in the microfluidic fabrication along with intersected applications at the fields of biology, medicine, and materials science, as well as together with well-aligned interactions between commercial vendors and end-users for further developments in hardware and software domains. All these potential improvements would be “game changers” to make microfluidics more accessible to both researchers and end-users in a variety of fields.

4. Sensor Integration

Besides a large versatility of material types in their fabrication, another excitement is the integrity of microfluidics with multiple platform technologies due to its modular design as a key compartment in platform development. Since microfluidics is an enabling technology for POC diagnostic tools, a vast majority of recently developed sensing modalities have benefitted from their microscale capability in terms of sampling, automation, control on minute volume scales, high-throughput, thereby amplifying their attention on the applications of POC diagnosis.^[204,205] In this section, the integration of advanced sensing modalities and smart technologies with microfluidic devices is reviewed profoundly.

4.1. Plasmonic and Photonic Sensors

While reducing material size into micro- and nanometric-scales, unique and striking modalities have often been unveiled in a large variety of materials, including plasmonic surfaces, nanoplasmonic noble particles, photonic crystals, and quantum dots.^[206–208] Their integration with enabling technologies such as microfluidics and their practical applications to real-world problems are of paramount significance for the scientific realm, technology, medicine, and industry. As an example, the collective oscillation state of conduction electrons on a metal surface creates a distinctive sensing phenomenon termed “surface plasmons.”^[209] Basically, these plasmonic materials are produced with a variety of metal surfaces (mostly gold and silver)^[210] along with altering surface geometries and combining different materials that form metamaterials. At the close vicinity of a metal surface, a local electromagnetic wave is generally amplified by a coupling unit, such as a prism, waveguide, and grating. Furthermore, surface plasmon frequency is monitored through absorption, scattering, transmission, and photoluminescence, enhancing its applicability to different sensing strategies.^[211,212] Particularly, planar metal-deposited surfaces, nanohole arrays, nanostructures, and nanocavities denoting umpteen applications in biomedical engineering, are primarily utilized in biosensing and clinical diagnostic purposes due to high sensitivity to the dielectric interface upon the binding of biotargets to the sensor surface.^[213] Considering the need for well-equipped infrastructure in the fabrication, researchers have recently focused on commercially available off-the-shelf, such as digital versatile discs (DVDs) and compact discs (CDs), being already designed as a slab array with a certain period and dimension.^[214] Despite all these features, we need to consider some obstacles including labor-intensive fabrication techniques, associated costs, the hindrance with a refractive index of biological samples, and surface passivation. All these points are still drawbacks for the frequent utilization of these sensors at POC settings.

On the other hand, noble nanoparticle-based methods—the other plasmonic phenomenon, trap the light wave within conductive nanoparticles comparable or smaller than the wavelength of light, thereby resulting in i) an enhancement of electric field at the close vicinity of the nanoparticle surface and ii) maximum optical absorption at the plasmon resonant

frequency.^[215] By constructing nanoplasmonic surfaces on-chip formats, researchers were able to detect a variety of biomolecules, cells, bacteria, and viruses from clinically-relevant fluids with high sensitivity.^[216–218] As a recent example, an opto-microfluidic platform was relied on the gold nanopikes fabricated by electrodeposition and integrated with a microfluidic chip.^[219] The platform was able to detect the presence (qualitative detection) and level of antibodies specific to the SARS-CoV-2 spike protein (quantitative detection) in 1:1 diluted human plasma samples (1 μL of human plasma and 1 mL of buffer solution) within around 30 min. With label-free detection, the platform was able to reach the detection limits down to around 0.08 ng mL^{-1} ($\approx 0.5 \times 10^{-12}$ M), which was lower than the clinical limit. Although the system was capable of real-time monitoring and low detection limit, it provided a restricted linear dynamic range around two or three orders of magnitude. Although ease-of-synthesis and diverse functionalization options make nanoparticle-type systems versatile in biosensing and diagnostic applications, colloidal stability can be interfered with harsh chemicals during functionalization, leading to particle aggregation in solution or on the surface. Many efforts have altered this undesired property into a naked-eye detection (e.g., juxtaposed aggregation, nanoparticle growth in size, and charge alteration), creating a nonconventional strategy that improves current ELISA-based assay performance.^[220,221] Recent outbreak, i.e., COVID-19 pandemic, has also increased the attention on the naked-eye detection strategies.^[222] For this manner, gold nanoparticles were modified with thiol-terminated antisense oligonucleotides (ASOs) targeting N-gene (nucleocapsid phosphoprotein) of SARS-CoV-2 and provided the results within 10 min. The strategy was very simple and effective through an agglomeration process when the target RNA was captured by the thiol-modified ASO-capped gold nanoparticles, and moreover, this agglomeration strategy was tuned and amplified with the addition of RNaseH that cleaved the RNA strand from the RNA–DNA hybrid, leading to a visually detectable precipitation. Selectivity was examined through the presence of MERS-CoV viral RNA, and the limit of detection was observed as 0.18 ng μL^{-1} of SARS-CoV-2 RNA.

One outstanding fashion of optical sensing systems is to unify multiple modalities with distinct detection strategies. As aforementioned, while applying them to biosensing purposes, all these procedures have critical bottlenecks, i.e., either the interference caused by inherent optical properties of biospecimens; the difficulties on the synthesis and modification of nanoparticles or the requirement of signal amplification. Obviously, these systems require more effort to bring multiple disciplines, including materials science, surface chemistry, and physics, and therefore, they provide very unique detection capabilities with low detection levels and high detection ranges.

4.2. Micro/Nanomechanical and Acoustic Sensors

Inspiration by unique machines in living organisms, such as mechanical sensing units in plants and human glabrous skin, have guided researchers to create micro- and nanomechanical devices that sense biological processes at cellular and molecular levels by measuring forces, displacements, and mass changes

in a variety of conditions with a single-molecule/single-cell sensitivity.^[223] These sensors can be mass-produced through standard wafer-scale semiconductor processing techniques. They measure the mass down to zeptogram-scale in vacuum and nanogram resolution in fluidic conditions;^[224] monitor minuscule forces in biological interactions down to ≈ 10 pN, and exhibit fast response times that enable to screen biological processes within the timescales of milliseconds.^[223] Principally, mechanical sensors can be classified into two major groups: i) Surface-stress mechanical sensors monitor the quasistatic deflection of a cantilever, caused by the binding events on a sensor surface. They are sensitive to monitor the binding of proteins^[225] and nucleic acids,^[226] as well as conformational changes^[227] and cellular motion for antibiotic testing of bacterial infections.^[228] ii) Dynamic-mode mechanical sensors (non-quasistatic) oscillate with a resonance frequency and measure minute changes when biotargets bind to a cantilever surface. These sensors can be operated in a humid/gas-phase and fluid-phase condition (detection in vacuo), as well as they, measure continuously in fluid and utilize suspended microchannel resonators.^[223]

We here highlight that an ideal biosensing strategy takes place in fluidic conditions in which biotarget and recognition units on the sensor properly interact with each other. Detection in a fluid is a simpler and direct measurement, but mechanical and acoustic sensing in situ is notably hindered by viscous damping.^[229] To circumvent this parasitic effect and achieve very low detection resolution on these sensors, a hybrid detection strategy, removing the sensor from fluid and detecting in vacuo, is applied. However, replacing and desiccating sensors makes these bioassays cumbersome and this strategy is prone to false-positive results due to measurement artifacts.^[223] Although labeling biotargets captured on the sensor help diminishing false-positive results, this increases assay time and cost, and requires labor-intensive operation by trained personnel that limit their deployment to the POC and point-of-need settings. Another bottleneck—not only for mechanical sensors, but also for the others, is nonspecific binding since the number/concentration of biotargets in biological specimens (e.g., serum, blood, and sputum) is many orders of magnitude lower than the other molecules, cells, and proteins in the sample. Although pre-concentration with or without concurrent immuno-affinity depletion can help to reduce the effect of nonspecific binding, sample processing is still a cumbersome step in the detection. To address these challenges, the ultimate mechanical sensors will ideally be integrated with precise microfluidic sample handling, multiplexing, and automation for complex processing protocols. Cells and cellular entities are, for instance, caged in microchannels with pico to nanoliter volumes,^[230] maintaining biotargets from individual cells that enable mechanistic control for biosensing in situ. As an example, a bi-material microcantilever was integrated with a microfluidic channel, which was functionalized with receptor molecules specific to bacteria passing through the channel.^[231] The platform provided two different detection modes: i) the captured bacteria inside the cantilever altered the resonance frequency due to their mass and also deflected the cantilever because of the adsorption stress; and ii) furthermore, the bacteria was excited through infrared radiation (IR) and thereby the cantilever was deflected due

to the proportion to the infrared absorption of the bacteria, denoting selectivity through a nanomechanical infrared spectrum. With this platform, the researchers demonstrated single bacterium detection per μL , and more examinations on antibiotic susceptibility were performed while exposing ampicillin and kanamycin to *Escherichia coli*, providing distinct responses to different anti-microbials.

In fact, the micro-/nanomechanical sensors have capabilities to detect a single organism or molecules, yet their laborious and expensive fabrication, extremely sensitive to the environment causing high background signals, and the need for specific conditions are remaining bottlenecks for these sensors. On the other hand, one of the most renowned and commercially available mechanosensors, i.e., quartz crystal microbalance (QCM), monitors the mass load on sensor surfaces in the conditions of gas, vacuum, or fluid by recording dumping in the resonant frequency in real-time.^[232] By utilizing dissipation mode, they can also track the alterations in the viscoelasticity of cellular membranes.^[232,233] Although QCM allows detecting biotargets in situ, the need for an isolation unit to minimize any vibrational forces and temperature changes is still a vital challenge for their deployments to the POC settings.

4.3. Electrochemical Sensing Modality

Quantification of biological or biochemical reactions is of utmost significance to convert the biological information to an easily processed electronic readout. Electrochemical sensors hold notable potential in this regard, and they have denoted a vast majority of biosensing applications, such as glucose sensors for daily-use, due to low-cost production, ease-of-use, portability, facile readout, and simplicity of sensor construction. Typically, they are inspected under three major means: i) amperometric readouts for a measurable current; ii) potentiometric measurements for a measurable electrical potential or charge accumulation; and iii) conductometric readouts for monitoring conductive properties of a medium between electrodes.^[234] Recent advances in this field have revived other electrochemical sensing strategies, including chronoamperometry, cyclic voltammetry, impedance spectroscopy, chronopotentiometry, nanowires, and field-effect transistor-stemmed systems.^[235]

Among other biosensing modalities, an enzyme is generally utilized as a core biological unit on electrochemical sensors in order to catalyze a biochemical reaction and generate an electrochemical signal. In addition, electrochemical nose/tongue approaches,^[236] affinity-based,^[237] and hybridization-based strategies^[238] are currently taking substantial attention since designing enzymatic reactions confine to broaden the applications of electrochemical sensors. For instance, a family of synthetic and biomolecular-functionalized graphene probes was designed as an array of electrochemical sensing system—chemical nose/tongue approach—to distinguish i) different cell types; ii) cancer cells, multidrug-resistant cancer cells, and metastatic human breast cells, and iii) artificial CTC samples with high accuracy.^[239] Principally, the sensor surface distinctly interacts with surfaces of divergent cell types, providing a blueprint to classify and distinguish different cells. Such differential affinity strategy was able to discern various cell types at

levels down to 100 cells, and also with a detection of a single-cell type. As another example, a microchannel card (μ -card) was decorated with a hybrid polymer nanofiber-multiwalled carbon nanotube (MWCNT) for selective determination of clinically relevant biomarkers (i.e., acetone and toluene) in exhaled breath from patients with lung cancer and diabetes.^[240] In this regard, our perspective is that combining a noninvasive sampling strategy into a hand-held detector system will potentially pave the way for the rapid detection of volatiles at POC diagnosis in high-risk group individuals as a screening test that would accelerate the early diagnosis of diseases.

The sensors reliant on the field-effect transistors provide high-sensitivity, label-free operation, and chip-scale construction. In particular, for this aspect, chemical vapor deposition graphene provides more flexibility to denote the applications of multiplexed DNA arrays because of its large 2D morphology readily and possibilities for the top-down fabrication of transistor arrays. However, DNA sensors reliant on graphene field-effect transistors have been usually employed at the single-device level. On the other hand, a study utilizing the chemical vapor deposition graphene and fabrication of field-effect transistor arrays with two features demonstrates a new strategy to develop multiplexed DNA arrays.^[241] With this design and strategy, the platform provided a sensitivity down to 100×10^{-15} M. Moreover, in the platform, each graphene acted as an electrophoretic electrode, where site-specific probe DNAs were decorated, and these electrodes performed specific detection of DNA targets on the field-effect transistor. Consequently, graphene as both electrode and transistor demonstrated a crucial step for multiplexed graphene-based DNA arrays. As another example, a graphene field-effect transistor was fabricated on Si/SiO₂ substrate to detect chlorpyrifos—one of the most utilized pesticides that impact the nervous system in humans, and the platform was designed to monitor any changes in electrostatic potential.^[242] For this purpose, anti-chlorpyrifos antibodies were first immobilized to the graphene surface, and the nonactivated areas on the sensor were passivated with bovine serum albumin in order to minimize any nonspecific binding from the real samples. The platform provided a linear dynamic range between fM and μ M, and it was able to detect the pesticide down to 1.8×10^{-15} M in the spiked samples, highlighting the utility of graphene field-effect transistors for the detection of pesticides in fruits and vegetables.

Despite all these remarkable features of the electrochemical sensors, we point out that conductivity caused by the nature of biospecimens is still one of the most significant challenges in their applications for clinical samples. A handful of years ago, researchers sought new strategies such as replacing conducting medium with nonconductive alternatives through a multi-step procedure, and then, they were able to isolate viral particles from blood and serum samples using antibody-coated magnetic particles.^[243] The captured biotargets were then washed and lysed with nonconductive solutions, and measured impedance values of viral lysates on interdigitated electrodes on-chip. The same group further applied this strategy with a multi-target format and altered the design into a printed electrode sensor on flexible plastics, thereby accelerating their access and utility for point-of-need settings.^[221] Despite the versatility in the sensor format, changing the medium with nonconductive solutions

and the associated procedure hinder its applicability to the POC settings, where untrained personnel run the experiment without any specialized, automated equipment.

5. Point-of-Care Diagnosis

Biological targets including viruses, bacteria, cells, proteins, metabolites, and nucleic acids circulate in bodily fluids such as blood, saliva, sweat, and urine.^[244] Detection of these biomolecules via microfluidic-based POC platforms has enabled rapid, user-friendly, reliable, and robust fashions in biomedical applications.^[245] As working principles and the required functional modules rely on biological targets, we elaborate on recent applications in the POC diagnostic platforms and categorize them into three major classes as proteins, whole cells, and nucleic acids in the following sections, as well as compared all the platforms according to their properties and analytic performance (Table 2).

5.1. Protein and Small Molecule Detection

Protein-based biomarkers are often employed for clinical diagnosis due to their easy access to bodily fluids. Proteins are well-known biological entities that are responsible for various biological functions ranging from enzymatic reactions to hormone synthesis, maintenance of metabolic equilibrium, and tissue repair.^[246] They are also one of the most important classes of POC biomarkers as their level often reflects the presence and/or status of certain diseases and disease stages that commonly need to be diagnosed.^[247]

In this context, as an example, Rusling's group introduced to combine microfluidics with an electrochemical sensor to achieve protein biomarkers of cancer.^[248] In this study, they used a molded PDMS channel, which was integrated with a pump and sample injector. They evaluated the platform with the detection of PSA and interleukin-6 through an assay sandwiching the target biomarkers between superparamagnetic particle-antibody conjugates and antibodies attached to an eight-electrode system. Overall, the superparamagnetic particles were conjugated with ≈ 90 K antibodies and 200 K horseradish peroxidase labels to obtain efficient off-line capture and high sensitivity, and the system reached the sensitivities of 0.23 pg mL^{-1} for prostate-specific antigen and 0.30 pg mL^{-1} for interleukin-6 in serum mixtures. On a parallel track, Sardesai et al. fabricated an electrochemiluminescence sensor, integrated with a microfluidic system in order to detect protein biomarkers (prostate-specific antigen and interleukin-6) from serum samples.^[249] The system employed three molded PDMS channels on a conductive pyrolytic graphite chip-inserted into a chamber and interfaced with a pump, switching valve, and sample injector. Each of the three PDMS channels encompassed three analytical wells. They also decorated single-wall carbon nanotube forests with capture antibodies at the bottom of the wells, and accordingly, captured target antigens. Ru(bpy)₃²⁺-silica-secondary antibody was then injected to label the captured antigens on the array, followed by the injection of sacrificial reductant tripropylamine to produce electrochemiluminescence. The chip was

Table 2. Evaluation of sensor types along with target molecules, specimen types, analytic performance, advantages, and disadvantages.

Sensor type	Detection strategy	Target	Specimen	Dynamic range	Limit of detection	Advantages	Disadvantages	Ref.
Electrochemical platform	<ul style="list-style-type: none"> Superparamagnetic particle attached antibody conjugates 	<ul style="list-style-type: none"> Prostate-specific antigen (PSA) Interleukin-6 (IL-6) 	<ul style="list-style-type: none"> Serum 	<ul style="list-style-type: none"> 0.225–20 pg mL⁻¹ (PSA) 0.30–20 pg mL⁻¹ (IL-6) 	<ul style="list-style-type: none"> 0.23 pg mL⁻¹ (PSA) 0.30 pg mL⁻¹ (IL-6) 	<ul style="list-style-type: none"> Good correlation with ELISA Sensitivity Multiplexed detection 	<ul style="list-style-type: none"> Lengthy assay time Multi-step procedure Low linear dynamic range 	[248]
Electrochemiluminescence platform	<ul style="list-style-type: none"> Antibody-decorated single-wall carbon nanotubes 	<ul style="list-style-type: none"> PSA IL-6 	<ul style="list-style-type: none"> Serum 	<ul style="list-style-type: none"> 100 fg mL⁻¹–10 ng mL⁻¹ (PSA) 10 fg mL⁻¹–1 ng mL⁻¹ (IL-6) 	<ul style="list-style-type: none"> 100 fg mL⁻¹ (PSA) 10 fg mL⁻¹ (IL-6) 	<ul style="list-style-type: none"> Good correlation with ELISA Sensitivity Low volume 	<ul style="list-style-type: none"> Multi-step procedure 	[249]
Electrochemical platform	<ul style="list-style-type: none"> Glutathione-decorated gold nanoparticles and antibody-decorated magnetic beads 	<ul style="list-style-type: none"> IL-6 IL-8 Vascular endothelial growth factor (VEGF) VEGF-C 	<ul style="list-style-type: none"> Serum 	<ul style="list-style-type: none"> ≈10–1000 fg mL⁻¹ 	<ul style="list-style-type: none"> 5 fg mL⁻¹ (VEGF and IL-6) 10 fg mL⁻¹ (IL-8) 50 fg mL⁻¹ (VEGF-C) 	<ul style="list-style-type: none"> Good correlation with ELISA Multiplexed assay Sensitivity Short assay time Clinical validation 	<ul style="list-style-type: none"> Need for signal amplification Need for sample preparation (capturing biotargets off-chip) 	[250]
Optical platform	<ul style="list-style-type: none"> Agarose beads-based sandwich immunoassay 	<ul style="list-style-type: none"> Biomarkers (CA125, HE4, MMP-7, and CA72-4) 	<ul style="list-style-type: none"> Serum Plasma 	<ul style="list-style-type: none"> 0–400 U mL⁻¹ (CA125) 0–200 pmol L⁻¹ (HE4) 0–50 U mL⁻¹ (CA72-4) 0–10 ng mL⁻¹ (MMP-7) 	<ul style="list-style-type: none"> 1.8 U mL⁻¹ (CA125) 2.3 pmol L⁻¹ (HE4) 1.7 U mL⁻¹ (CA72-4) 0.2 ng mL⁻¹ (MMP-7) 	<ul style="list-style-type: none"> Multiplexed detection Modular design High specificity Low cross-reactivity Short assay time 	<ul style="list-style-type: none"> Need for a bulky instrument Multi-step procedure Low linear dynamic range 	[251]
Electrochemical platform	<ul style="list-style-type: none"> Standard sandwich immunoassay 	<ul style="list-style-type: none"> IL-6 Abelson tyrosine kinase 	<ul style="list-style-type: none"> Serum (50% of human serum) 	<ul style="list-style-type: none"> 5 × 10⁻⁵–5 × 10⁻¹¹ M (IL-6) 1 × 10⁻⁷–1 × 10⁻¹³ M (Abelson tyrosine kinase) 	<ul style="list-style-type: none"> 50 × 10⁻¹² M (IL-6) 100 × 10⁻¹² M (Abelson tyrosine kinase) 	<ul style="list-style-type: none"> Multi-target detection Multi-step procedure Low linear dynamic range Lack of clinical validation 	<ul style="list-style-type: none"> Lengthy assay time 	[252]
Optical platform	<ul style="list-style-type: none"> Protease-sensitive peptide substrates liberated from carrier nanoparticles 	<ul style="list-style-type: none"> Thrombin 	<ul style="list-style-type: none"> Urine 	<ul style="list-style-type: none"> ≈1–7 × 10⁻⁹ M 	<ul style="list-style-type: none"> 1 × 10⁻⁹ M 	<ul style="list-style-type: none"> Visual detection Facile operation Clinical validation Multiplexed fashion in vivo Data collection from ELISA and LFA 	<ul style="list-style-type: none"> Multi-step procedure Low linear dynamic range Need for a bulky instrument 	[253]
Paper-based platform	<ul style="list-style-type: none"> Aptamer crosslinked hydrogels Enzymatic cascade reactions 	<ul style="list-style-type: none"> Cocaine 	<ul style="list-style-type: none"> Urine (50% of urine) 	<ul style="list-style-type: none"> 0–400 × 10⁻⁶ M 	<ul style="list-style-type: none"> 3.8 × 10⁻⁶ M 	<ul style="list-style-type: none"> Low-cost Facile operation Disposable system Portability Visual detection 	<ul style="list-style-type: none"> Signal amplification Multi-step procedure Low linear dynamic range Lack of clinical validation 	[254]
Optical platform	<ul style="list-style-type: none"> Streptavidin-modified bars 	<ul style="list-style-type: none"> Biotin 	<ul style="list-style-type: none"> Whole blood 	<ul style="list-style-type: none"> 1.5 × 10⁻¹² M–1.5 × 10⁻⁶ M 	<ul style="list-style-type: none"> 1.5 × 10⁻¹² M 	<ul style="list-style-type: none"> Short assay time Self-powered system No need for external valves or pumps Low sample volume Use of unprocessed sample Disposable system Facile operation 	<ul style="list-style-type: none"> Lack of biomarker detection Lack of clinical validation 	[255]

Table 2. Continued.

Sensor type	Detection strategy	Target	Specimen	Dynamic range	Limit of detection	Advantages	Disadvantages	Ref.
Optical platform	<ul style="list-style-type: none"> Catalase conjugated silica nanoparticles functionalized with ELISA detection antibodies 	<ul style="list-style-type: none"> Catalase 	<ul style="list-style-type: none"> PBS Culture Serum Urine 	<ul style="list-style-type: none"> 3–30 U mL⁻¹ 	<ul style="list-style-type: none"> Not reported 	<ul style="list-style-type: none"> Quantitative Multiplexed detection Equipment-free system Clinical validation 	<ul style="list-style-type: none"> High number of cells are needed to meet the detection limit Multi-step procedure 	[256]
Optical platform	<ul style="list-style-type: none"> Cold-conjugated antibodies 	<ul style="list-style-type: none"> HIV biomarkers Syphilis biomarkers 	<ul style="list-style-type: none"> Whole blood 	<ul style="list-style-type: none"> Not reported 	<ul style="list-style-type: none"> Not reported 	<ul style="list-style-type: none"> Facile operation Low-cost Clinical validation Field study 	<ul style="list-style-type: none"> Multi-step procedure Need for signal amplification 	[257]
Optical platform	<ul style="list-style-type: none"> Loop-mediated isothermal amplification 	<ul style="list-style-type: none"> DNA 	<ul style="list-style-type: none"> Not reported 	<ul style="list-style-type: none"> 10–10⁵ fg μL⁻¹ 	<ul style="list-style-type: none"> 10 fg μL⁻¹ 	<ul style="list-style-type: none"> Multiplexed detection Low sample volume Isothermal condition 	<ul style="list-style-type: none"> Customized probe design for each biotarget Lack of clinical validation 	[265]
Optical platform	<ul style="list-style-type: none"> Isothermal recombinase polymerase amplification 	<ul style="list-style-type: none"> DNA 	<ul style="list-style-type: none"> Buffer solution 	<ul style="list-style-type: none"> 2–200 copies 	<ul style="list-style-type: none"> <10 copies 	<ul style="list-style-type: none"> High energy efficiency Short assay time 	<ul style="list-style-type: none"> Need for a benchtop instrument Lack of multiplexing 	[266]
Optical platform	<ul style="list-style-type: none"> Loop-mediated isothermal amplification 	<ul style="list-style-type: none"> DNA 	<ul style="list-style-type: none"> Pathogens (<i>Streptococcus agalactiae</i>, koi herpes virus, Iridovirus, <i>Aeromonas hydrophila</i>) 	<ul style="list-style-type: none"> Not reported 	<ul style="list-style-type: none"> 20 copies 	<ul style="list-style-type: none"> Multiplexed detection Short assay time 	<ul style="list-style-type: none"> Need for an additional assay for the detection of samples 	[267]
Optical platform	<ul style="list-style-type: none"> Neutrophil functional assay 	<ul style="list-style-type: none"> Neutrophils 	<ul style="list-style-type: none"> Whole blood 	<ul style="list-style-type: none"> Not reported 	<ul style="list-style-type: none"> Not reported 	<ul style="list-style-type: none"> Short assay time Low sample volume Facile operation Clinical validation 	<ul style="list-style-type: none"> Need for a benchtop instrument 	[273]
Electrochemical platform	<ul style="list-style-type: none"> Antimicrobial peptide-based detection 	<ul style="list-style-type: none"> <i>Streptococcus sanguinis</i> 	<ul style="list-style-type: none"> KCl solution Artificial saliva 	<ul style="list-style-type: none"> 10¹–10⁶ CFU mL⁻¹ 	<ul style="list-style-type: none"> 10² CFU mL⁻¹ 	<ul style="list-style-type: none"> Short assay time Label-free fashion Sensitivity 	<ul style="list-style-type: none"> Need for a benchtop instrument for the detection Lack of clinical validation 	[274]
Optical platform	<ul style="list-style-type: none"> ZnO nanorod - integrated microdevice 	<ul style="list-style-type: none"> Avian influenza virus 	<ul style="list-style-type: none"> PBS 	<ul style="list-style-type: none"> 3.6 × 10²–3.6 × 10⁶ EID₅₀ mL⁻¹ 	<ul style="list-style-type: none"> 3.6 × 10³ EID₅₀ mL⁻¹ 	<ul style="list-style-type: none"> Multiplexed detection Flexibility Portability Low-cost 	<ul style="list-style-type: none"> Multi-step procedure Lack of clinical validation 	[275]

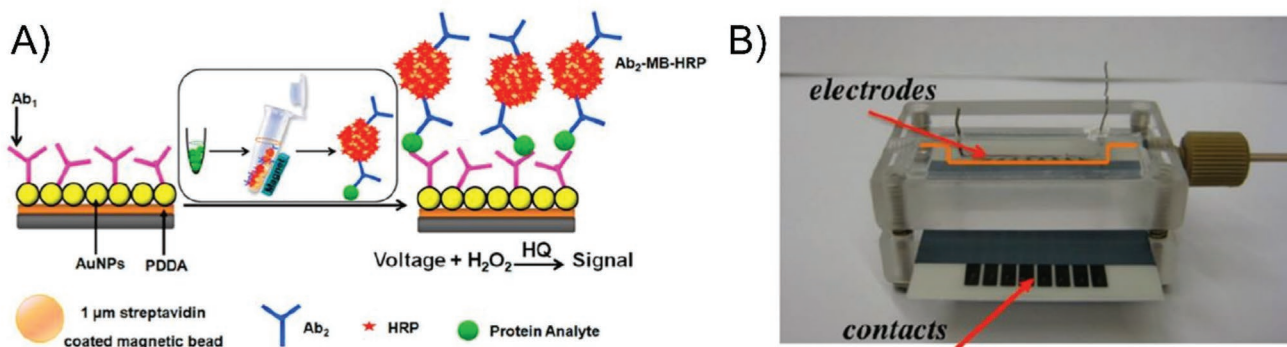


Figure 3. An electrochemical sensing method on the microfluidics. A) A single sensor along with the detailed surface chemistry agents and detection strategy, and B) the eight-sensor immunoarray decorated with the capture antibodies. Reproduced with permission.^[250] Copyright 2012, American Chemical Society.

placed into an open-top electrochemiluminescence, measuring the levels of protein biomarkers down to 100 fg mL^{-1} for prostate-specific antigen and 10 fg mL^{-1} for interleukin-6 in calf serum. Another study was reported to employ an electrochemical microfluidic system for measuring four protein biomarkers (Figure 3).^[250] The system had an eight-electrode electrochemical workstation integrated with a microfluidic array system that measured amperometric changes for the detection. The microfluidic chip was produced with the molded PDMS on the top of the electrode array made of eight carbon screen-printed electrodes with $700 \mu\text{m}$ of diameter. The sealing was enabled with two PMMA plates, and the top PMMA plate was designed for the integration of tubings and electrodes (Ag/AgCl: reference electrode and Pt: counter electrode). The electrodes were coated with poly(diallyl dimethylammonium chloride) (PDDA), and they were further modified with glutathione-decorated gold nanoparticles, where the primary antibodies were immobilized via a surface chemistry approach. The biomarkers were captured with secondary antibody-decorated magnetic beads, having streptavidin and horseradish peroxidase complex, and the captured biomarkers were then isolated using a magnet. These isolated biomarkers were then applied to the electrode system, and this study was further validated a protein panel for accurate oral cancer diagnostics, resulting in an ultralow detection limit ($5\text{--}50 \text{ fg mL}^{-1}$) for simultaneous measurement of protein biomarkers including interleukin 6 (IL-6), interleukin 8 (IL-8), vascular endothelial growth factor (VEGF), and vascular endothelial growth factor C (VEGF-C) in diluted serum. They also showed a clinical sensitivity of 89% and specificity of 98% for oral cancer detection in patient serum and control samples, signifying the multiplexed feature of this system and applicability in biospecimens.

Multiplexed biomarker protein detection holds unrealized promise for clinical cancer diagnostics due to lack of suitable measurement devices and lack of rigorously validated protein panels. As an example, an ultrasensitive electrochemical microfluidic array were optimized to measure a four-protein panel of biomarker proteins, and validated with a protein panel for accurate oral cancer diagnostics. Unprecedented ultralow detection into the $5\text{--}50 \text{ fg mL}^{-1}$ range was achieved for simultaneous measurement of proteins IL-6, IL-8, VEGF, and VEGF-C in diluted serum. The immunoarray achieves high sensitivity in 50 min assays by using off-line protein capture by mag-

netic beads carrying 400 000 enzyme labels and 120 000 antibodies. After capturing the proteins and washing to inhibit nonspecific binding, the beads are magnetically separated and injected into the array for selective capture by antibodies on eight nanostructured sensors. Good correlations were received with ELISA results for protein determinations in conditioned cancer cell media, and this further confirmed the accuracy of this approach. Normalized means of the 4-protein levels in 78 oral cancer patient serum samples and 49 controls resulted in clinical sensitivity 89% and specificity 98% for oral cancer detection, demonstrating high utility in diagnosis. Inexpensive, low cost, easily-fabricated immunoarray provides a rapid serum test for diagnosis and personalized therapy of oral cancer. The device is readily adaptable to clinical diagnostics of other cancers.

As an example of another multiplexed platform, a programmable microfluidic platform was reported for the detection of distinct biomarkers (CA125, HE4, MMP-7, and CA72-4).^[251] Their programmable microfluidic platform relied on a bead immuno-analyzer system, which was combined with automated sample metering, bubble and debris removal, reagent storage, and waste disposal, and the system was further miniaturized to the size of a credit card. The platform was validated with the patient cohorts encompassing early- and late-stage ovarian cancer along with benign and healthy controls. As a result, the platform was able to distinguish the stages from control samples with 68.7% of sensitivity at 80% of specificity. Continuing from the multifaceted features of microfluidic systems, Mok et al. presented a digital on-chip platform for protein biomarker detection, where the portable platform accommodates the integrated electronics to handle minute sample volume ($<5 \mu\text{L}$) (Figure 4).^[252] In this configuration, the system was superior able to sense interleukin-6 samples down to $50 \times 10^{-12} \text{ M}$ with at least six orders of magnitude linear dynamic range, which was than that of ELISA results. They further evaluated the system with Abelson tyrosine kinase activity in the presence of as low as $100 \times 10^{-12} \text{ M}$ of the kinase.

In another study, exogenous agents serving as synthetic biomarkers were employed to detect urinary signals.^[253] The platform included the synthetic biomarkers composing nanoparticles, which were conjugated to ligand-encoded reporters via protease-sensitive peptide substrates. Upon delivery, the nanoparticles migrate to the diseased spots passively, such as solid

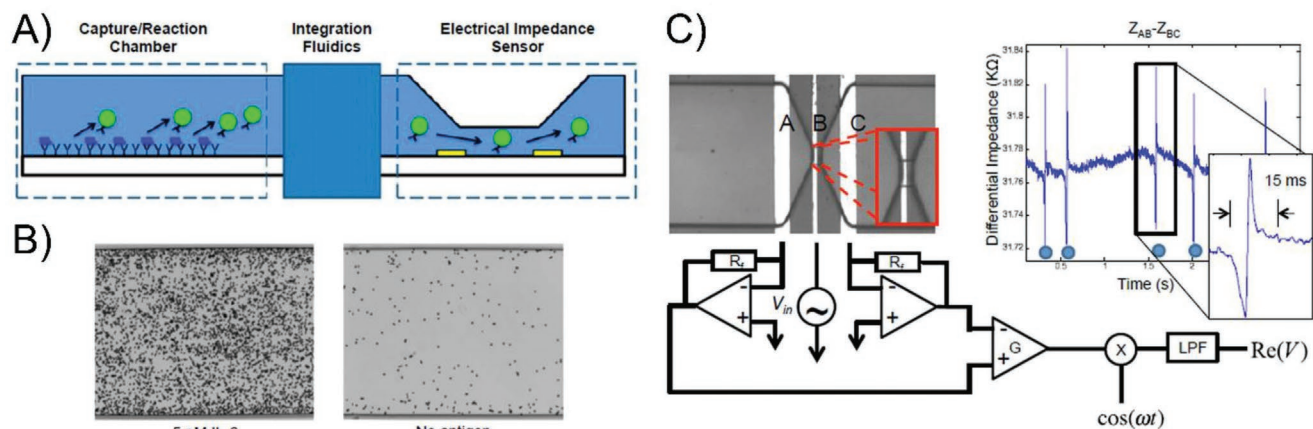


Figure 4. A) Scheme of the microfluidic platform. B) The images of specifically bound beads in the capture/reaction chamber. C) The image and technical design of an electrical impedance sensor. Reproduced with permission.^[252] Copyright 2014, Proceedings of the National Academy of Sciences of the United States of America.

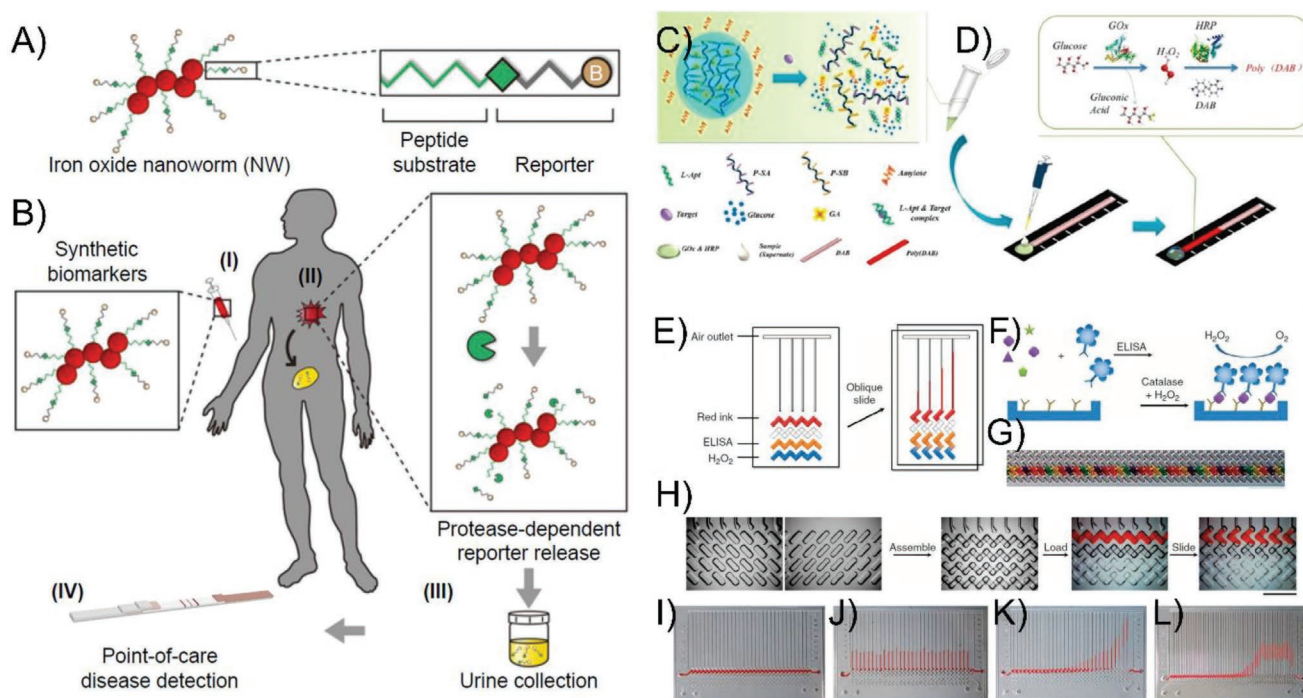


Figure 5. A) A schematic for the production of synthetic biomarkers. B) The proteolytic cleavage of the linking peptide-based substrate releases the ligand-encoded reporters, passing into urine; I) a patient with a suspected disease receives a mixture containing of a disease-tuned diagnostic nanoworm, II) nanoworms migrate to the disease site and release the reporters once proteolytic cleavage of peptide substrates occurs, III) the patient provides a urine sample, IV) point-of-care paper is employed to detect the disease from unprocessed urine samples. Reproduced with permission.^[253] Copyright 2014, Proceedings of the National Academy of Sciences of the United States of America. C) Target recognition enables dissolution of the hydrogel to liberate glucoamylase for catalyzing the formation of a large amount of glucose. D) The conversion of glucose to gluconic acid catalyzed by glucose oxidase (GOx) enables hydrogen peroxide (H_2O_2), which reacts with 3,3'-diaminobenzidine (DAB) with the catalysis of horseradish peroxidase (HRP) that yields a brown poly(DAB) stripe in microfluidic paper-based system. Reproduced with permission.^[254] Copyright 2016, American Chemical Society. E) The schematic representation of a typical volumetric bar-chart sensor F) volumetric bar-chart sensor ELISA reaction and the oxygen formation mechanism, G) an image of 50 sample-wells which are loaded with different colored food dyes using swab tips, H) the magnified images of bottom and top plates, device assembly, reagent loading and assay operation, I) an image demonstrating the 30-plexed volumetric bar-chart sensor loaded with the red ink and reagents, J) a uniform ink advancement image showing the application of equal concentrations of catalase, and K, L) progressive ink advancement in 30- and 50-channel sensor generated by the 3- and 6-h diffusion of catalase from the inlet ports. Reproduced with permission.^[255] Copyright 2012, Nature Publishing Group.

tumors or blood clots, where up-regulated proteases cleaved the peptide substrates and liberated the reporters that were cleared into the urine (Figure 5A,B). With further adaptation into a paper diagnostic strategy, the researchers tailored the synthetic biomarkers, targeting specifically to both colorectal cancer (a representative solid tumor) and thrombosis (a common cardiovascular disorder), and they achieved to detect these maladies in mouse models using their urine samples as low as $\approx 1 \times 10^{-9}$ M within a working linear range of $\approx 1-7 \times 10^{-9}$ M.

Other than a paper format, microfluidic platforms have been constructed in a hydrogel-paper system for the detection of small molecules such as cocaine.^[254] In this case, the researchers synthesized the hydrogel with trapped glucoamylase using an aptamer as a crosslinker, and monitored the collapsing behavior of hydrogel and consequently the release of glucoamylase into the sample, which was followed by the formation of glucose through amyolysis (Figure 5C,D). Here, they modified the channel with glucose oxidase and 3,3'-diaminobenzidine as the substrate. Accordingly, glucose traveled along the channel through the capillary action, and it was then converted to hydrogen peroxide by glucose oxidase. Moreover, 3,3'-diaminobenzidine was converted into brown insoluble poly-3,3'-diaminobenzidine by horseradish peroxidase, producing a visible brown bar, whose length was positively correlated to the concentration of targets as a quantitative measurement of cocaine in urine samples. The platform was designed on a cascade reaction detecting down to 3.8×10^{-6} M of cocaine, and it would be potentially applied to the quantification of other molecules by designing specific aptamers to the target of interest.

In addition, a self-powered, integrated microfluidic blood analysis system was developed to analyze blood.^[255] This system required a minute volume of whole-blood only, and it was able to remove red and white blood cells, followed by analyte detection in platelet-containing plasma. Within 10 min, the system achieved a sensitivity down to 1.5×10^{-12} M with 99.9–100% of blood cell retention in the passive structure. Moreover, Song et al. presented a multiplexed volumetric bar-chart sensor, denoting an easy-to-use platform that provides quantitative results without the need for optical instruments or any data processing steps.^[256] Through measuring oxygen production by catalase activity, which was proportional to the concentration of the analyte, the researchers measured the displacement of ink along the channels. Rapid quantification of protein biomarkers in diverse clinical samples was also evaluated using this volumetric bar-chart sensor (Figure 5E–L). Another integrated on-chip system facilitated the fluid handling and signal detection on a single platform called “mChip” assay, which was further validated with HIV samples collected in Rwanda.^[257] In this design, the researchers achieved to detect HIV biomarkers using only 1 μ L of unprocessed whole blood, as well as diagnosed both AIDS and syphilis with high sensitivities and specificities that were comparable to the performance of benchtop platforms. The platform provided facile sampling and multiplexed detection strategy. Briefly, the chip surface was coated with specific antigens to HIV and syphilis, and then the patient's whole blood was introduced to the chip. According to the presence of antibodies against these infections, the antigen-antibody complex was then labeled with gold-conjugated antibodies and the signal was further amplified the reduction

of silver ions on gold nanoparticles, providing both quantitative and qualitative (naked-eye) detection.

As aforementioned, protein, antibody, or small molecule biomarkers have been utilized extensively in the microfluidic platforms, which are reliant on conventional PDMS-type, paper format, and hydrogel-integrated systems. Proteins are small in size yet more informative agents in disease or health status, as well as their circulation in the bloodstream or urine, make them great candidates in noninvasive or semiinvasive diagnostics.^[258,259] Despite their facile sampling and high specificity, proteins, antibodies, or small molecule biomarkers might be hindered by the external factors easily, thereby altering their 3D structures, and they are no longer detected by the recognition elements on the microfluidic chips. Therefore, the materials used in microfluidic chips need to offer a biocompatible milieu for the detection. Moreover, due to their small sizes, proteins, antibodies, or small molecules can easily adhere to nonactivated sites, reducing the yield efficiency and potentially minimizing the detection performance of the sensor on a microfluidic chip. Antifouling agents help to address this drawback by improving the specificity and also yield capture and detection efficiency at the same time.^[260] All these points need to be considered before detecting these biomarkers in any type of microfluidic and sensor platforms.

5.2. Nucleic Acid Detection

Nucleic acids—intracellular carriers of genetic information, play vital roles in any biomolecular status or disease, as well as they join circulation to transfer information to other tissues/organs in the body.^[261–263] Simply putting into words, microfluidic-based diagnostic tools detecting nucleic acid biomarkers focus to monitor the concentrations of deoxyribonucleic acid (DNA) or ribonucleic acid (RNA) in order to assay particular genetic details of a patient; or to assay nucleic acid sequences, which are unique to invade pathogens, thereby providing an important opportunity for rapid purification of nucleic acids from blood.^[264] As a basic principle, target sequences from the sample are captured on a substrate surface, where specific probes are immobilized to form a hybridization process that is then converted into readable signals via any optical or magnetic reporters.^[244] As an example, Fang et al. depicted a micro-loop-mediated isothermal amplification system that was designed as an eight-channel microfluidic sensor.^[265] The readout was performed either by the naked-eye or by measuring absorbance values through an optical sensor. Within an hour, the platform was able to analyze target sequences quantitatively with high sensitivity (10 fg of DNA) and specificity under isothermal conditions.

On a parallel track, Lutz et al. demonstrated a lab-on-a-foil system for nucleic acid detection through the strategy of isothermal recombinase polymerase amplification (Figure 6A,B).^[266] Interestingly, this system was based on a foil-based centrifugal microfluidic cartridge that was produced by blow-molding and sealed with a self-adhesive tape. The cartridge was combined with the pre-stored liquid and dried reagents for the fluorescence detection in real-time. They characterized the system with an assay for the detection of the antibiotic resistance gene *mecA* of *Staphylococcus aureus*. A capillary siphon and a centrifugo-pneumatic valve were integrated for

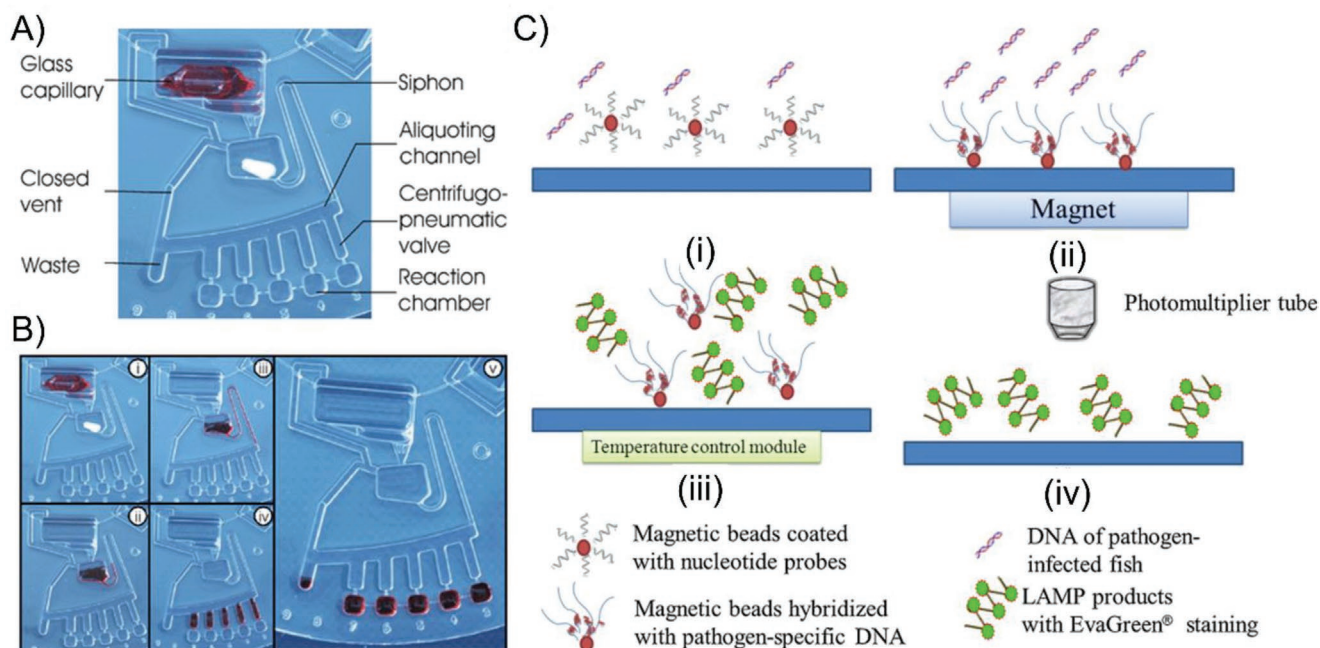


Figure 6. A) The photograph of the microfluidic cartridge containing a foil disc, which is composed of a chamber with a glass capillary and another chamber with a lyophilisate. B) The step-wise process of the disc is demonstrated. Reproduced with permission.^[266] Copyright 2010, the Centre National de la Recherche Scientifique (CNRS) and The Royal Society of Chemistry. C) Schematic representation of the workflow in the loop-mediated isothermal amplification (LAMP) on-chip. The system provides several application and sample manipulations, including i) thermal lysis and hybridization, ii) isolation of pathogen DNA while applying an external magnetic field, iii) LAMP reaction, and iv) optical detection. Reproduced with permission.^[267] Copyright 2013, Elsevier.

the fluid control, and in this system, the limit of detection was observed less than ten copies for <20 min. Microfluidic unit operations enabled the storage and release of liquid reagents, reconstitution of lyophilized reagents, aliquoting the sample into independent reaction cavities, and the mixing of reagents with the DNA samples. According to the report, this system outperformed the PCR-based platforms in terms of energy efficiency and time-to-result parameters.

Browsing with some examples in the literature, an integrated microfluidic system was developed to detect DNA molecules of biotargets captured on magnetic beads followed by the loop-mediated isothermal amplification process (Figure 6C).^[267] Their system consisted of closed microvalves, micropumps, loop-mediated isothermal amplification reaction chambers, and wash units, pointing out that the entire process was able to be performed for the isolation of pathogen DNA, nucleic acid amplification, and optical detection of the products. This system could automatically complete the entire process within 65 min with a detection limit of 20 copies. The system performance was also benchmarked with the detection of four different pathogens (*Streptococcus agalactiae*, Koi herpes virus (KHV), Iridovirus, and *Aeromonas hydrophila*) simultaneously.

Overall, detecting nucleic acids requires extensive isolation systems to prepare the samples; and also needs precise temperature control and specific enzymatic reactions under specialized temperatures. However, these are significant caveats that limit their applicability to the POC settings. Isothermal amplification reaction, on the other hand, provides a unique capability to operate these reactions at a single temperature with high efficiency.^[268] Operating isothermal reactions on a microfluidic platform offers multiplexing on a small region, as well as helps

stability in temperature control. Moreover, with transparent materials, the microfluidic platforms provide a naked-eye detection for such nanosized and a rare number of nucleic acids easily.^[269] In addition to the isothermal reactions, the probes can be immobilized to the microfluidic chips through specific surface chemistry, e.g., avidin–biotin or chemical linking strategies. However, steric hindrance is still a problem since the sequence of nucleic acid needs to be within a distance from the surface for efficient hybridization with the target sequence. In this scenario, polymeric materials or tethering molecules/structures like lipid bilayers^[270] exhibit dynamic behavior to the probe molecules, hence addressing this challenge.^[271,272] Despite their high specificity for disease diagnostics, nucleic acids are fragile biomaterials, and they require more sophisticated microfluidic systems for precise sample manipulations. This does not only increase the assay cost and also leads to remarkable complexity, limiting their operations to the research laboratories mostly, and therefore, these factors minimize their utility and applicability to the resource-constrained settings.

5.3. Whole-Cell and Virus Detection

Cells and viruses are the repertoires of protein, nucleic acid, lipid, and carbohydrate biomarkers, and they provide critical information on disease diagnostics, disease pathology, tracking the infection and drug efficacy for clinical research, biological warfare, disease outbreaks, and food safety. Moreover, this information is further validated with downstream analyses, such as genomics, transcriptomic, and proteomics for the fundamental research. For instance, Tay et al. reported a microfluidic-based

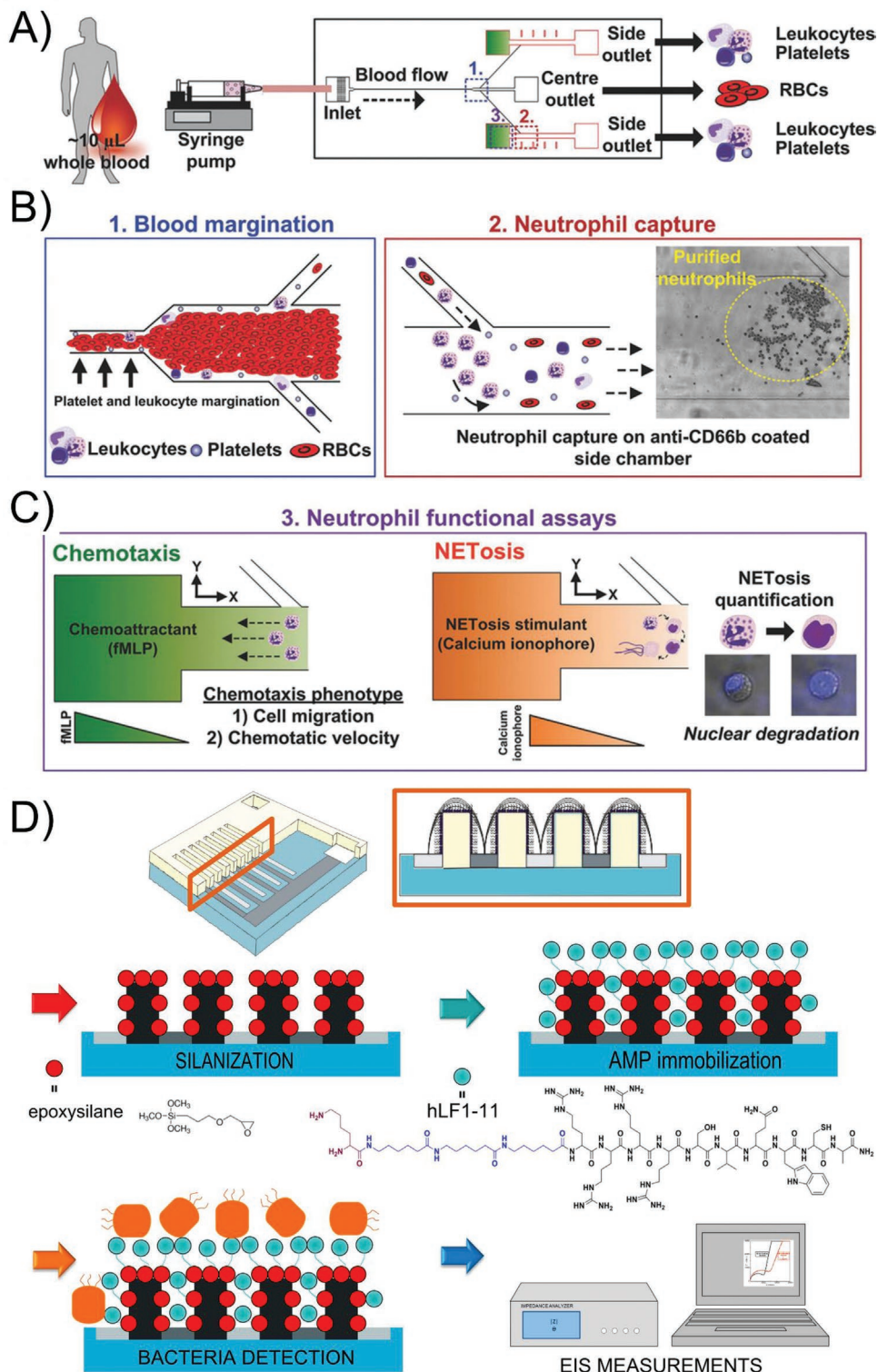


Figure 7. A) The workflow of the microfluidic platform for neutrophil sorting and functional characterization. B) Neutrophil purification via a two-step procedure. C) Neutrophil functional assay is performed through either preloaded chemoattractant, i.e., *N*-formylmethionyl-leucyl-phenylalanine, or calcium ionophore. Therefore, on-chip chemotaxis and formation of neutrophil extracellular trap assay is carried out. Reproduced with permission.^[273] Copyright 2018, John Wiley and Sons. D) Schematic demonstration of the platform and the surface functionalization of the 3D interdigitated electrode array for the bacterial detection (*Streptococcus sanguinis*). Reproduced with permission.^[274] Copyright 2016, Elsevier.

platform for neutrophil sorting and phenotyping (chemotaxis and formation of neutrophil extracellular traps) by employing low blood volumes (Figure 7A–C).^[273] In this manner, they purified neutrophils on-chip from whole blood directly using biomimetic cell margination and affinity-based capture, and followed by this step, they exposed the cells to preloaded chemoattractant or chemotaxis and formation of neutrophil extracellular traps stimulant, respectively. After that, they characterized the platform performance by applying healthy and in vitro inflamed blood samples (clinical risk stratification in a cohort of subjects with type 2 diabetes mellitus). Herein, they reported that “high-risk” type 2 diabetes mellitus patients characterized by severe chemotaxis impairment revealed significantly higher C-reactive protein levels and poor lipid metabolism characteristics compared to “low-risk” subjects. Moreover, their neutrophil chemotaxis responses might be mitigated after in vitro metformin treatment. Thus, their microfluidic-based platform enabled the quantification of chemotaxis and formation of neutrophil extracellular traps in medical applications, and it would be further converted into a tool for risk stratification and precision methods in subjects with metabolic diseases.

As another example, Hoyos-Nogués et al. aimed to develop a miniaturized microfluidic platform for monitoring *Streptococcus sanguinis*—one of the most prevalent strains in the onset of periodontal diseases (Figure 7D).^[274] In this manner, they synthesized potent antimicrobial peptides derived from human lactoferrin and covalently immobilized them on interdigitated electrode arrays. Following the immobilization, they used X-ray photoelectron spectroscopy and electrochemical impedance spectroscopy to optimize and characterize the immobilization. Moreover, they performed the interaction of *S. sanguinis* with antimicrobial peptide-coated platforms and obtained significant changes in the impedance spectra, which were associated with the presence of bacteria. According to the results, the platform was able to detect the bacteria at concentrations starting from 10^1 colony forming units (CFU) mL⁻¹ in KCl and 10^2 CFU mL⁻¹ in artificial saliva. They also carried out the lacking cytotoxicity of the system for human fibroblasts.

In addition to whole-cell detection, a nanorod-integrated microfluidic platform was developed for the detection of avian influenza virus.^[275] This system was able to detect viruses specifically within 1.5 h and provided a low limit of detection value as 3.6×10^3 EID₅₀ mL⁻¹ (EID₅₀: 50% embryo infectious dose) which was almost 22 times more sensitive than the conventional enzyme-linked immunosorbent assay. Moreover, this microfluidic-based platform enabled to detect multiple viruses simultaneously by the spatial encoding of capture antibodies and provided an alternative tool as a multiplexed pathogen detection tool, potentially broadening to the other medical applications with impactful fashions (e.g., low-cost and easy-to-use) for POC settings.

Overall, conventional and standard methods of whole-cell and virus detection are often laborious, and turnaround time takes several hours to days.^[276] From the perspective of POC applications, along with analytical performance (sensitivity and specificity), facile user interpretation, stability under operating conditions, preferably portability and disposability are required.^[277,278] While focusing on whole-cell and virus detection, we still need to consider all these check-points.

6. Overview: Strengths and Limitations of Microfluidics and POC Systems

As elaborated with the recent advances in the literature, microfluidics has leveraged the existing POC platforms in terms of low-sample volume, easy manipulation of fluids, nearly limitless integration with any types of sensor, efficient cell sorting and isolation, as well as enabling tissue/organ environment along with managing shear and flow parameters as existing in the native milieu of cells. Despite their significance in this realm, the success of POC applications is directly proportional to the material used. Although several attempts have been done, and many successful results have been reported for the integration of materials into microfluidic systems, there is still no perfect material, which is widely applicable to all applications at the POC settings. Since developing materials for these systems requires multidisciplinary efforts, continuous coordination of different fields, such as engineering and biological and physical sciences, are needed to develop new materials, yet all produced materials come with its own strength and limitations. To choose the right material for the suitable system has own checkpoints.

The materials that reviewed in this review are organized in four main categories along with their intrinsic limitations. The first group of materials includes inorganic materials, e.g., glass, silica, and ceramic materials. Although these materials have high chemical stability, high thermoconductivity, well-characterized surface and insulating properties, and high aspect ratio forming microchannels, high costs associated with their fabrication impede their deployments into the field. Due to their fragile and brittle properties, these kinds of materials are difficult to process and create components like valves and pumps for multi-functionality in microfluidics.^[279] In addition, since harsh chemicals are used during the processing stages of silica-based materials, well-protective facilities, specific training, and well-implemented restrictions to use these chemicals are required.^[280] Beside these impediments, inorganic materials other than glass are opaque, and therefore, they are not useful for microfluidic systems, which are integrated with optical sensing systems, such as plasmonic or fluorescence modalities. Despite the suitability of glass for optical sensing systems, it is prone to breakage and more expensive than other inorganic materials.^[281] Another obstacle that must be overcome for the deployment of inorganic materials is to increase their oxygen permeability. Especially, in the cell and tissue engineering-related research, oxygen permeability is one of the vital parameters that cells can exchange gas from the external environment, yet this is an existing challenge in the use of inorganic materials in microfluidics.^[282] The second group refers polymeric materials, such as hydrogels, PDMS, polyfluoropolyethers, PMMA, PS, cyclic-olefin copolymer (COC), and SU-8. Highlighting their major features, polymers can i) resist mechanical shocks; ii) remain transparent at most wavelengths; iii) they are disposable and biocompatible, iv) require less stringent cleaning techniques; and v) show greater oxygen permeability than inorganic materials. However, these materials mostly show low resistance to organic solvents, and especially, when aggressive and polar aprotic solvents are used for filtration, they cannot be used in food, biotechnology and pharmaceutical industry

processes.^[283] Since the production efficiency of soft lithography-stemmed methods is very low, they are not suitable for these applications, and also, easy evaporation of water from polymer surfaces can lead to the loss of samples when such materials are employed.^[284,285] Among the other polymers, hydrogels also display similar limitations, but their analytical properties such as sensitivity, specificity, and detection threshold can be improved with new strategies and advanced technologies.^[286] Besides, polymer materials like PDMS are not rough or rugged enough, and they hence cause some issues on the flow profile, such as leakage or pressure differences in the microfluidic system.^[287] The third group consists of paper materials, and they denote many advantages such as highly porous matrix, low-cost, ease-of-assembly, integration of multiple operation units, disposability, easy storage of reagents in the channel, and facile readout. Paper materials are however opaque, and similar to silica materials, they cannot be employed easily in optical sensing systems, particularly in transmission-based measurements and also in fluorescence-based measurements due to their high background signal, interfering the measurements potentially. On the other hand, the nonuniformity and batch-to-batch variations due to their intrinsic features are notable impediments. Even, on the same area of a paper, fibers and textures differ from each other, dramatically reducing their accuracy in terms of sensitivity and the wicking rates of liquids.^[288] Another difficulty can be mentioned as coffee-ring effect, which is the tendency of solutes to accumulate toward the outer edges of the paper while they dry. This issue leads to nonhomogeneous distribution of analytes, reaction products, or reagents in the liquid that directly affects the results. Apart from the coffee effect, drying liquids on the paper also reduce their shelf-life and activity, because the drying reagents, such as enzymes, significantly lose their activity, and they must be re-hydrated each time before their operation, which require more preprocessing steps and time.^[289–291] The final group is carbonaceous materials, including CNTs and graphene. These materials have remarkable properties such as ultrasensitivity in sensing systems, inexpensive production, easy functionality, high electrical and thermal conductivity, high aspect ratio, chemical and mechanical stability, and super hydrophobicity. Mentioning their limitations in the field, graphene-based systems, for instance, have not turned into a well-known product in this area yet since there is no well-standardized and facile way to obtain graphene.^[292,293] In addition, due to the close interactions with biological entities, CNT and graphene need to meet biocompatibility aspects fully before their implementation. As reported in the literature,^[294–297] CNTs are trapped in the respiratory system when inhaled directly, and consequently, they increase pulmonary inflammation by causing lung fibrosis after their accumulation here.

The POC systems are indicated as an alternative testing or near-patient testing, and they perform bio-analytical tests outside centralized laboratories. This strategy has been implemented for many diseases and health monitoring facets. In this regard, POC systems have been benefitted extensively from biosensors and microprocessors, and since the last decades, we have witnessed the integration of microfluidic platform with these systems. In principle, POC systems along with the complement platforms like microfluidics exhibit many advantages,

including shorter turnaround times, low sample volume, easy-to-use, potential reduction in workload at hospitals, more rapid clinical decisions, and more frequent monitoring/screening the health status or treatment. Despite their well-defined highlights, there are some check-points that need to be addressed for a clear clinical benefit.

At the first glance, sampling at the pre-analytical phase is the first check-point that requires appropriate sample handling and collection procedure to minimize sampling-related errors.^[298] The sampling also needs to be facile for the use of noninvasive or semiinvasive strategies. In addition, the biomarkers or analytes of interest need to be exist in the samples to match the correlated concentrations that are measured in the clinical laboratories. In this manner, sometimes, sampling at the pre-analytical phase require some pre-processing steps to enrich the biomarker concentration in the specimen, especially in the complex matrices like blood, urine, saliva, or lavage fluid. This step minimizes the interference notably caused by the intrinsic parameters of bio-matrices, such as abundance of different cells, proteins and lipids.^[299] In addition to preprocessing, the stabilization of clinical samples with chemicals enables precise measurements.^[298,300,301] The implementation of these systems to resource-constrained settings or personalized medicine perspective is hampered by such extensive procedures along with multi-step tasks and enrichment devices that lead to complexity and increase the assay cost remarkably. Second, handling and maintenance of analyzers is key to obtain accurate results at every measurement, and therefore, we would have comparable results with the gold standard methods for proper clinical decision. Third, other than home-settings or bed-side, the implementation site of POC systems could span from emergency rooms, intensive care units, or operating rooms in a hospital to the primary care units or satellite outpatient clinics.^[302] The staff members at hospital and clinic focus predominantly on clinical care, and however, the training of clinical staff operating POC systems might be challenging in a such large network. Regular quality controls and ongoing competency maintenance of the staff need to be ubiquitous. Fourth, in addition to the management of training, calibration and maintenance of the POC systems need to be implemented regularly. In principle, POC systems have low-complexity, yet they are designed in specialized modalities. Any malfunctions in their mechanical/electrical components hamper to obtain reliable results, and hence, regular control with trained personnel is an obvious need. Fifth, POC systems provide results in either qualitative or quantitative ways. Qualitative means are very helpful for untrained individuals, but the threshold of the positive results needs to be well-defined considering the clinical decision of the disease. On the other hand, quantitative results provide more information and enable easy monitoring on the levels of biomarkers at different time slots; however, sensitivity and selectivity of this reporting type need to be well-established with the gold standard method. There is a critical need for further development and benchmarking these systems in order to reduce false negatives and or false positives that provide the results comparable to the methods operated at the centralized laboratories.^[298,303–305] To secure specificity, any possibilities causing to false positives need to be minimized or eliminated through application of antifouling agents that protects the nonactivated

sites on the system from nonspecific binding in bio-matrices. In addition, increasing the sensitivity can enable high precision in detection and monitor the levels of analytes even at low concentrations. In this regard, signal-to-noise (SNR) plays a vital role during the translation of sensor performance by reducing the noise and increasing the signal, and this can enable to measure the minute alterations in the signals, hence leading to a lower limit-of-detection. Signal amplification is one way of tuning the SNR, yet it increases the number of steps and time to perform the assay, and generally, it is not a cost-efficient because of the addition of expensive equipment and/or reagents to the system. On the other hand, increasing the density of recognition elements targeting the analytes of interest is another way to improve the sensitivity, and the cost-associated challenges however still exist. Sixth, the stability of reagents decorated on the system is another critical parameter, and enhancing their stability can prolong the shelf-life, especially for long-term storage and also implementing them into resource-constrained settings. Although antibodies provide great affinity to analytes, they are interfered by external factors like temperature changes and humidity. Artificial antibodies, i.e., molecularly imprinted polymers (MIPs), would be an alternative strategy to overcome from this issue since they provide specific molecular grooves of target analytes, and hence, mimic probe-analyte interactions.^[306] Due to their polymeric nature of MIPs, they can also prolong the shelf-life and enable longer-term stability. However, current imprinting strategies need to be revisited to increase catalytic capability and sufficient selectivity and affinity to the target analytes. All these aspects impact on the accuracy of measurement, and a high-fidelity process during the development of MIPs could help to solve these existing challenges.^[298] Seventh, multiplexing provides a very wide window on evaluating the health status of an individual through screening several parameters at the same time. However, the readout hardware at the POC systems often has poorer performance than those at the centralized laboratories considering the cost and facile use by the end-user. Moreover, interference between different detection slots need to be avoided for proper interpretation of the results, and this might be solved by integrating several sensors that monitor the signals at the specified sites only. Nevertheless, while improving the multiplexing capability, we still need to consider the assay cost and user-interface for the POC settings. Eighth parameter is the required energy for proper operation of the system. Especially, in resource-constrained settings, the power supply is a key element, and in most scenarios, the paucity of electrical source hampers the operation, and also, might cause to significant technical problems in the hardware. In principle, a POC system is composed of sample handling unit, sensor unit, signal processing, and data acquisition, and nearly all these units require power for the appropriate operation. In this regard, battery-operated systems are garnered more attention as having external power supplies, yet their regular maintenance and replacement after long-term use is the critical challenge to deploy them into these settings. There are some efforts to integrate rechargeable batteries to minimize these needs, and however, the toxicity of these batteries (lithium, mercury, lead, and cadmium) is still an obstacle. There are recent efforts to implement solar, mechanical, or bio-fuel based energy sources to the POC systems, lowering the needs for power and at the same time providing continuous

and bio-friendly operation.^[298,307–309] Ninth, POC systems have been not integrated with any documentation systems since they are performed by individuals. This may lead to insufficient documentation and difficult comparability of the results obtained in routine clinical tests.^[310] Last years, we have experienced the integration of cloud systems and the analysis of the results through online medical platforms, and they would be important directions to minimize these issues efficiently.^[311]

7. Conclusion

The significance of POC devices has been much appreciated during the paradigm shift in the health care system from centralized care to home-based diagnostic platforms since these devices offer facile use and sampling, short turnaround time, portability, and high accuracy. In particular, their implementation in developing countries with huge populations has an immense impact on reducing the health-associated costs and reducing the workload at hospitals. During this transition, especially, microfluidics has impacted greatly on POC devices through the fabrication of business-card size and automated systems via conventional, yet continuously updated procedures by using a small number of materials and low reagent consumption. Moreover, these small devices require only a drop of biospecimen, which can be taken by individuals with very basic training like finger pricking or collecting urine. Hence, these unique characteristics have garnered the attention of many researchers to use microfluidics in POC devices for many fields, especially in disease diagnostic purposes. However, at the beginning of microfluidics research, the designed POC devices were not considered and focused more on the perspective of end-users, they were more likely academic research-stemmed studies. Therefore, these devices could not make enough impact on any demanded products in the field. Recent efforts harmonized by engineers, biologists, chemists, materials scientists, physicists, and medical doctors have not only altered the fabrication methods due to the notable need for biocompatibility and inherent features of biospecimens, but also have provided new strategies for the functionality of microfluidic devices. At the same time, these mutual interactions have enabled them to exchange their views in order to make standardized protocols for mass productions, thereby accelerating their deployment as POC diagnostic tools. Such interactions have made it possible to produce inexpensive, accurate, more specific, sensitive, and more end-user-oriented systems on the industrial-scale. Moreover, microfluidics has very flexible properties with nearly unlimited integrations of materials and sensors, thereby signifying its broad use to multiple fields. There are also some checkpoints for microfluidics and POC systems that need to be re-visited before their translation and utilization into the bed-side, home-setting, hospitals, and physician offices. We here list them as material type, physical and chemical characteristics, optical features, oxygen permeability, resistance to harsh chemicals, flow profile, porous matrix, cost, ease-of-assembly, integration of multiple operation units, disposability, easy storage of reagents in the channel, facile readout, batch-to-batch production, shelf-life, easy functionality, electrical and thermal conductivity, high aspect ratio, handling and maintenance of analyzers, training,

calibration, sensitivity, specificity, multiplexing, power supply, and documentation of the results. Due to immense efforts in the field, we easily foresee that the existing platforms will be updated accordingly. For instance, we face pandemics more frequently in the 21st century, and health systems need more advance and new technologies more than ever for a quick and accurate diagnosis to prevent the spreading of diseases to the communities. Of course, while facing new medical challenges like today's pandemic or ongoing health issues such as fertilization problems,^[312] microfluidics would provide new solutions through mutual integration with sensor systems, accelerating their adaptation to our daily routines for early diagnosis of diseases and treatment monitoring, as well as improving the sample processing in research laboratories such as forensic applications.^[313–315]

Acknowledgements

Dr. Fatih Inci gratefully acknowledges the support from the Scientific and Technological Research Council of Turkey (TÜBİTAK) 2232-International Fellowship for Outstanding Researchers (Project No: 118C254) and TÜBİTAK 3501-Career Development Program (CAREER) (Project No: 120Z335). This publication was produced benefiting from the 2232 International Fellowship for Outstanding Researchers Program of TÜBİTAK (Project No: 118C254). However, the entire responsibility of the publication/paper belongs to the owner of the publication/paper. The financial support received from TÜBİTAK does not mean that the content of the publication is approved in a scientific sense by TÜBİTAK. Drs. Yeşeren Saylan and Fatih Inci are grateful to TÜBİTAK for the financial support through 1001-The Scientific and Technological Research Projects Funding Program (Project No: 120Z445). Dr. Garbis Atam Akceoglu gratefully acknowledges the support from TÜBİTAK 2218-National Postdoctoral Research Fellowship Program for Turkish Citizens. This work was supported by the BAGEP Award of the Science Academy.

Conflict of Interest

The authors declare no conflict of interest.

Keywords

biosensors, diagnostics, integrated sensors, microfluidics, point-of-care, smart materials

Received: January 17, 2021
Revised: April 11, 2021
Published online: May 9, 2021

- [1] S. L. Gutierrez, T. E. Welty, *Ann. Pharmacother.* **2004**, *38*, 119.
- [2] L. C. J. Clark, C. Lyons, *Ann. N. Y. Acad. Sci.* **1962**, *102*, 29.
- [3] The History of the Pregnancy Test Kit, A Timeline of Pregnancy Testing, **2014**.
- [4] A. St John, C. P. Price, *Clin. Biochem. Rev.* **2014**, *35*, 155.
- [5] A. J. Singer, J. Ardise, J. Gulla, J. Cangro, *Ann. Emerg. Med.* **2005**, *45*, 587.
- [6] M. Kankaanpää, M. Raitakari, L. Muukkonen, S. Gustafsson, M. Heitto, A. Palomäki, K. Suojanen, V.-P. Harjola, *Scand. J. Trauma Resusc. Emerg. Med.* **2016**, *24*, 125.

- [7] G. J. Kost, *Arch. Pathol. Lab. Med.* **2001**, *125*, 1307.
- [8] F. A. Meier, B. A. Jones, *Arch. Pathol. Lab. Med.* **2005**, *129*, 1262.
- [9] N. Convery, N. Gadegaard, *Micro Nano Eng.* **2019**, *2*, 76.
- [10] C. D. Chin, V. Linder, S. K. Sia, *Lab Chip* **2012**, *12*, 2118.
- [11] G. M. Whitesides, *Nature* **2006**, *442*, 368.
- [12] D. J. Beebe, G. A. Mensing, G. M. Walker, *Annu. Rev. Biomed. Eng.* **2002**, *4*, 261.
- [13] M. A. Alyassin, S. Moon, H. O. Keles, F. Manzur, R. L. Lin, E. Hæggestrom, D. R. Kuritzkes, U. Demirci, *Lab Chip* **2009**, *9*, 3364.
- [14] P. S. Dittrich, A. Manz, *Nat. Rev. Drug Discovery* **2006**, *5*, 210.
- [15] J. West, M. Becker, S. Tombrink, A. Manz, *Anal. Chem.* **2008**, *80*, 4403.
- [16] G. M. Whitesides, *Lab Chip* **2011**, *11*, 191.
- [17] H. A. Stone, A. D. Stroock, A. Ajdari, *Annu. Rev. Fluid Mech.* **2004**, *36*, 381.
- [18] P. Abgrall, A.-M. Gué, *J. Micromech. Microeng.* **2007**, *17*, R15.
- [19] D. Mark, S. Haeberle, G. Roth, F. von Stetten, R. Zengerle, *Chem. Soc. Rev.* **2010**, *39*, 1153.
- [20] J. Puigmartí-Luis, *Chem. Soc. Rev.* **2014**, *43*, 2253.
- [21] K. Choi, A. H. C. Ng, R. Fobel, A. R. Wheeler, *Annu. Rev. Anal. Chem.* **2012**, *5*, 413.
- [22] A. Manz, N. Graber, H. M. Widmer, *Sens. Actuators, B* **1990**, *1*, 244.
- [23] D. J. Harrison, A. Manz, Z. Fan, H. Luedi, H. M. Widmer, *Anal. Chem.* **1992**, *64*, 1926.
- [24] J. Baek, P. M. Allen, M. G. Bawendi, K. F. Jensen, *Angew. Chem., Int. Ed.* **2011**, *50*, 627.
- [25] I. R. Baxendale, S. V. Ley, C. D. Smith, G. K. Tranmer, *Chem. Commun.* **2006**, 4835.
- [26] A. R. Wu, N. F. Neff, T. Kalisky, P. Dalerba, B. Treutlein, M. E. Rothenberg, F. M. Mburu, G. L. Mantalas, S. Sim, M. F. Clarke, S. R. Quake, *Nat. Methods* **2014**, *11*, 41.
- [27] A. Manz, D. J. Harrison, E. M. J. Verpoorte, J. C. Fetters, A. Paulus, H. Lüdi, H. M. Widmer, *J. Chromatogr. A* **1992**, *593*, 253.
- [28] E. Sollier, C. Murray, P. Maoddi, D. Di Carlo, *Lab Chip* **2011**, *11*, 3752.
- [29] E. Berthier, E. W. K. Young, D. Beebe, *Lab Chip* **2012**, *12*, 1224.
- [30] J. C. McDonald, D. C. Duffy, J. R. Anderson, D. T. Chiu, H. Wu, O. J. Schueller, G. M. Whitesides, *Electrophoresis* **2000**, *21*, 27.
- [31] J. C. McDonald, G. M. Whitesides, *Acc. Chem. Res.* **2002**, *35*, 491.
- [32] A. D. Stroock, G. M. Whitesides, *Acc. Chem. Res.* **2003**, *36*, 597.
- [33] S. K. Sia, G. M. Whitesides, *Electrophoresis* **2003**, *24*, 3563.
- [34] I. E. Araci, S. R. Quake, *Lab Chip* **2012**, *12*, 2803.
- [35] R. Mukhopadhyay, *Anal. Chem.* **2007**, *79*, 3248.
- [36] J. Zhou, H. Yan, K. Ren, W. Dai, H. Wu, *Anal. Chem.* **2009**, *81*, 6627.
- [37] K. Ren, Y. Zhao, J. Su, D. Ryan, H. Wu, *Anal. Chem.* **2010**, *82*, 5965.
- [38] M. E. Stewart, M. J. Motala, J. Yao, L. B. Thompson, R. G. Nuzzo, *Proc. Inst. Mech. Eng., Part N: J. Nanoeng. Nanosyst.* **2006**, *220*, 81.
- [39] S. Halldorsson, E. Lucumi, R. Gomez-Sjoberg, R. M. T. Fleming, *Biosens. Bioelectron.* **2015**, *63*, 218.
- [40] M. Mehling, S. Tay, *Curr. Opin. Biotechnol.* **2014**, *25*, 95.
- [41] M.-H. Wu, S.-B. Huang, G.-B. Lee, *Lab Chip* **2010**, *10*, 939.
- [42] K. Masahiro, L. Xiaofeng, K. Choongik, H. Michinao, B. J. Wiley, H. Donhee, W. G. Whitesides, *Adv. Mater.* **2010**, *22*, 2749.
- [43] S. Cheng, Z. Wu, *Lab Chip* **2010**, *10*, 3227.
- [44] S. Xu, Y. Zhang, L. Jia, K. E. Mathewson, K.-I. Jang, J. Kim, H. Fu, X. Huang, P. Chava, R. Wang, S. Bhole, L. Wang, Y. J. Na, Y. Guan, M. Flavin, Z. Han, Y. Huang, J. A. Rogers, *Science* **2014**, *344*, 70.
- [45] R. J. Jackman, T. M. Floyd, R. Ghodssi, M. A. Schmidt, K. F. Jensen, *J. Micromech. Microeng.* **2001**, *11*, 263.
- [46] H. Becker, C. Gartner, *Anal. Bioanal. Chem.* **2008**, *390*, 89.
- [47] Y. Zheng, W. Dai, D. Ryan, H. Wu, *Biomicrofluidics* **2010**, *4*, 036504.
- [48] A. Bertsch, P. Renaud, *Micromachines* **2015**, *6*, 790.
- [49] C. G. Khan Malek, *Anal. Bioanal. Chem.* **2006**, *385*, 1362.
- [50] S. Arscott, *Lab Chip* **2014**, *14*, 3668.

- [51] M.-P. Schmidt, A. Oseev, C. Engel, A. Brose, B. Schmidt, S. Hirsch, *J. Sens. Sens. Syst.* **2016**, 5, 55.
- [52] K. Ren, W. Dai, J. Zhou, J. Su, H. Wu, *Proc. Natl. Acad. Sci. USA* **2011**, 108, 8162.
- [53] A. Alrifaiy, O. A. Lindahl, K. Ramser, *Polymers* **2012**, 4, 1349.
- [54] P. M. van Midwoud, A. Janse, M. T. Merema, G. M. M. Groothuis, E. Verpoorte, *Anal. Chem.* **2012**, 84, 3938.
- [55] D. J. Throckmorton, T. J. Shepodd, A. K. Singh, *Anal. Chem.* **2002**, 74, 784.
- [56] R. B. Fair, *Microfluid. Nanofluid.* **2007**, 3, 245.
- [57] X. Hu, Y. Dong, Q. He, H. Chen, Z. Zhu, *J. Chromatogr. B: Anal. Technol. Biomed. Life Sci.* **2015**, 990, 96.
- [58] C.-W. Tsao, D. L. DeVoe, *Microfluid. Nanofluid.* **2009**, 6, 1.
- [59] C. Neils, Z. Tyree, B. Finlayson, A. Folch, *Lab Chip* **2004**, 4, 342.
- [60] E. M. Ahmed, *J. Adv. Res.* **2015**, 6, 105.
- [61] E. Katmiwati, T. Nakanishi, *Macromol. Res.* **2014**, 22, 731.
- [62] Y. K. Jung, J. Kim, R. A. Mathies, *Anal. Chem.* **2015**, 22, 3165.
- [63] C. B. Goy, R. E. Chaile, R. E. Madrid, *React. Funct. Polym.* **2019**, 145, 104314.
- [64] I. Willner, *Acc. Chem. Res.* **2017**, 50, 657.
- [65] K. Y. Lee, D. J. Mooney, *Chem. Rev.* **2001**, 101, 1869.
- [66] V. F. Sechrist, Y. J. Miao, C. Niyibizi, A. Westerhausen-Larson, H. W. Matthew, C. H. Evans, F. H. Fu, J. K. Suh, *J. Biomed. Mater. Res.* **2000**, 49, 534.
- [67] G. Molinaro, J. C. Leroux, J. Damas, A. Adam, *Biomaterials* **2002**, 23, 2717.
- [68] P. Bulpitt, D. Aeschlimann, *J. Biomed. Mater. Res.* **1999**, 47, 152.
- [69] Y. Qiu, K. Park, *Adv. Drug Delivery Rev.* **2012**, 47, 49.
- [70] M. Ibrahim, M. K. Richardson, *Reprod. Toxicol.* **2017**, 73, 292.
- [71] M. T. Logun, N. S. Bisel, E. A. Tanasse, W. Zhao, B. Gunasekera, L. Mao, L. Karumbaiah, *J. Mater. Chem. B* **2016**, 4, 6052.
- [72] D. Choi, E. Jang, J. Park, W. G. Koh, *Microfluid. Nanofluid.* **2008**, 5, 703.
- [73] W. G. Koh, M. Pishko, *Sens. Actuators, B* **2005**, 106, 335.
- [74] M. Ikeda, R. Ochi, I. Hamachi, *Lab Chip* **2010**, 10, 3325.
- [75] J. M. Ayuso, R. Monge, A. Martínez-González, M. Virumbrales-Muñoz, G. A. Llamazares, J. Berganzo, A. Hernández-Lain, J. Santolaria, M. Doblaré, C. Hubert, J. N. Rich, P. Sánchez-Gómez, V. M. Pérez-García, I. Ochoa, L. J. Fernández, *J. Neuro-Oncol.* **2017**, 19, now230.
- [76] S. W. Han, S. Lee, J. Hong, E. Jang, T. Lee, W. G. Koh, *Biosens. Bioelectron.* **2013**, 45, 129.
- [77] A. G. Lee, D. J. Beebe, S. P. Palecek, *Biomed. Microdevices* **2012**, 14, 247.
- [78] A. D. Powers, B. Liu, A. G. Lee, S. P. Palecek, *Analyst* **2012**, 137, 4052.
- [79] Y. Piao, D. J. Han, M. R. Azad, M. Park, T. S. Seo, *Biosens. Bioelectron.* **2015**, 65, 220.
- [80] A. Hatch, D. M. Pesko, S. K. Murthy, *Anal. Chem.* **2012**, 84, 4618.
- [81] R. Z. Lin, A. Hatch, V. G. Antontsev, S. K. Murthy, J. M. Melero-Martin, *Tissue Eng., Part C* **2015**, 21, 274.
- [82] P. Sajeesh, A. K. Sen, *Microfluid. Nanofluid.* **2014**, 17, 1.
- [83] K. Ren, J. Zhou, H. Wu, *Acc. Chem. Res.* **2013**, 46, 2396.
- [84] F. Kotz, K. Plewa, W. Bauer, N. Schneider, N. Keller, T. Nargang, D. Helmer, K. Sachsenheimer, M. Schafer, M. Worgull, C. Greiner, C. Richter, B. E. Rapp, *Adv. Mater.* **2016**, 28, 4646.
- [85] R. F. Shepherd, J. C. Conrad, S. K. Rhodes, D. R. Link, M. Marquez, D. A. Weitz, J. A. Lewis, *Langmuir* **2006**, 22, 8618.
- [86] J.-W. Kim, A. S. Utada, A. Fernandez-Nieves, Z. Hu, D. A. Weitz, *Angew. Chem., Int. Ed. Engl.* **2007**, 46, 1819.
- [87] L.-Y. Chu, A. S. Utada, R. K. Shah, J.-W. Kim, D. A. Weitz, *Angew. Chem., Int. Ed. Engl.* **2007**, 46, 8970.
- [88] R. K. Shah, H. C. Shum, A. C. Rowat, D. Lee, J. J. Agresti, A. S. Utada, L. Y. Chu, J. W. Kim, A. Fernandez-Nieves, C. J. Martinez, D. A. Weitz, *Mater. Today* **2008**, 11, 18.
- [89] R. M. Tiggelaar, F. Benito-López, D. C. Hermes, H. Rathgen, R. J. M. Egberink, F. G. Mugele, D. N. Reinhoudt, A. van den Berg, W. Verboom, H. J. G. E. Gardeniers, *Chem. Eng. J.* **2007**, 131, 163.
- [90] E. Samiei, M. Tabrizian, M. Hoorfar, *Lab Chip* **2016**, 16, 2376.
- [91] W. Shen, M. Li, C. Ye, L. Jiang, Y. Song, *Lab Chip* **2012**, 12, 3089.
- [92] W. Du, L. Li, K. P. Nichols, R. F. Ismagilov, *Lab Chip* **2009**, 9, 2286.
- [93] E. S. Fakunle, I. Fritsch, *Anal. Bioanal. Chem.* **2010**, 398, 2605.
- [94] M. R. Gongora-Rubio, P. Espinoza-Vallejos, L. Sola-Laguna, J. J. Santiago-Avilés, *Sens. Actuators, A* **2001**, 89, 222.
- [95] A. Vasudev, A. Kaushik, K. Jones, S. Bhansali, *Microfluid. Nanofluid.* **2013**, 14, 683.
- [96] K. Malecha, D. G. Pijanowska, L. J. Golonka, W. Torbic, *Sens. Actuators, B* **2009**, 141, 301.
- [97] N. Ibáñez-García, C. S. Martínez-Cisneros, F. Valdés, J. Alonso, *TrAC, Trends Anal. Chem.* **2008**, 27, 24.
- [98] P. Ciosek, K. Zawadzki, J. Łopacińska, M. Skolimowski, P. Bembnowicz, L. J. Golonka, Z. Brzózka, W. Wróblewski, *Anal. Bioanal. Chem.* **2009**, 393, 2029.
- [99] P. Bembnowicz, M. Małodobra, W. Kubicki, P. Szczepańska, A. Górecka-Drzazga, J. Dziuban, A. Jonkisz, A. Karpiewska, T. Dobosz, L. Golonka, *Sens. Actuators, B* **2010**, 150, 715.
- [100] A. Vasudev, A. Kaushik, Y. Tomizawa, N. Norena, S. Bhansali, *Sens. Actuators, B* **2013**, 182, 139.
- [101] L. Mou, X. Jiang, *Adv. Healthcare Mater.* **2017**, 6, 1601403.
- [102] C.-M. Cheng, A. W. Martinez, J. Gong, C. R. Mace, S. T. Phillips, E. Carrilho, K. A. Mirica, G. M. Whitesides, *Angew. Chem., Int. Ed. Engl.* **2010**, 49, 4771.
- [103] A. W. Martinez, S. T. Phillips, M. J. Butte, G. M. Whitesides, *Angew. Chem., Int. Ed. Engl.* **2007**, 46, 1318.
- [104] M. M. Hamed, A. Ainla, F. Guder, D. C. Christodouleas, M. T. Fernandez-Abedul, G. M. Whitesides, *Adv. Mater.* **2016**, 28, 5054.
- [105] M. S. Verma, M.-N. Tsaloglou, T. Siskey, D. Christodouleas, A. Chen, J. Milette, G. M. Whitesides, *Biosens. Bioelectron.* **2018**, 99, 77.
- [106] C.-C. Wang, J. W. Hennek, A. Ainla, A. A. Kumar, W.-J. Lan, J. Im, B. S. Smith, M. Zhao, G. M. Whitesides, *Anal. Chem.* **2016**, 88, 6326.
- [107] Z. Nie, C. A. Nijhuis, J. Gong, X. Chen, A. Kumachev, A. W. Martinez, M. Narovlyansky, G. M. Whitesides, *Lab Chip* **2010**, 10, 477.
- [108] A. W. Martinez, S. T. Phillips, G. M. Whitesides, E. Carrilho, *Anal. Chem.* **2010**, 82, 3.
- [109] E. Roy, A. Pallandre, B. Zribi, M.-C. Horny, F.-D. Delapierre, A. Cattoni, J. Gamby, A.-M. Haghiri-Gosnet, *Advances in Microfluidics*, IntechOpen, Rijeka **2016**.
- [110] Y. Lu, W. Shi, L. Jiang, J. Qin, B. Lin, *Electrophoresis* **2009**, 30, 1497.
- [111] E. Carrilho, A. W. Martinez, G. M. Whitesides, *Anal. Chem.* **2009**, 81, 7091.
- [112] S. Wang, T. Chinnasamy, M. A. Lifson, F. Inci, U. Demirci, *Trends Biotechnol.* **2016**, 34, 909.
- [113] D. M. Cate, J. A. Adkins, J. Mettakoonpitak, C. S. Henry, *Anal. Chem.* **2015**, 87, 19.
- [114] Y. He, Y. Wu, J.-Z. Fu, W.-B. Wu, *RSC Adv.* **2015**, 5, 78109.
- [115] Y. Yazdani, A. Roohi, J. Khoshnoodi, F. Shokri, *Avicenna J. Med. Biotechnol.* **2010**, 2, 207.
- [116] M. Dou, D. C. Dominguez, X. Li, J. Sanchez, G. Scott, *Anal. Chem.* **2014**, 86, 7978.
- [117] N. K. Thom, K. Yeung, M. B. Pillion, S. T. Phillips, *Lab Chip* **2012**, 12, 1768.
- [118] J. Hu, S. Q. Wang, L. Wang, F. Li, B. Pingguan-Murphy, T. J. Lu, F. Xu, *Biosens. Bioelectron.* **2014**, 54, 585.
- [119] T. Tian, J. Li, Y. Song, L. Zhou, Z. Zhu, C. J. Yang, *Lab Chip* **2016**, 16, 1139.
- [120] A. C. Glavan, R. V. Martinez, E. J. Maxwell, A. B. Subramaniam, R. M. D. Nunes, S. Soh, G. M. Whitesides, *Lab Chip* **2013**, 13, 2922.

- [121] A. C. Glavan, R. V. Martinez, A. B. Subramaniam, H. J. Yoon, R. M. D Nunes, H. Lange, M. M. Thuo, G. M. Whitesides, *Adv. Funct. Mater.* **2013**, *24*, 60.
- [122] C. I. L. Justino, T. A. P. Rocha-Santos, A. C. Duarte, T. A. P. Rocha-Santos, *TrAC, Trends Anal. Chem.* **2013**, *45*, 24.
- [123] P. Joseph, C. Cottin-Bizonne, J.-M. Benoit, C. Ybert, C. Journet, P. Tabeling, L. Bocquet, *Phys. Rev. Lett.* **2006**, *97*, 156104.
- [124] M. Ma, R. M. Hill, *Curr. Opin. Colloid Interface Sci.* **2006**, *11*, 193.
- [125] K. B. Mogensen, M. Chen, K. Molhave, P. Boggild, J. P. Kutter, *Lab Chip* **2011**, *11*, 2116.
- [126] A. Venkatanarayanan, K. Crowley, E. Lestini, T. E. Keyes, J. F. Rusling, R. J. Forster, *Biosens. Bioelectron.* **2012**, *31*, 233.
- [127] A. Rasooly, H. A. Bruck, Y. Kostov, *Methods Mol. Biol.* **2013**, *949*, 451.
- [128] M. A. Ali, P. R. Solanki, S. Srivastava, S. Singh, V. V. Agrawal, R. John, B. D. Malhotra, *ACS Appl. Mater. Interfaces* **2015**, *7*, 5837.
- [129] P. He, V. Oncescu, S. Lee, I. Choi, D. Erickson, *Anal. Chim. Acta* **2013**, *759*, 74.
- [130] M. A. Ali, S. Srivastava, P. R. Solanki, V. Reddy, V. V. Agrawal, C. Kim, R. John, B. D. Malhotra, *Sci. Rep.* **2013**, *3*, 2661.
- [131] F. C. Moraes, R. S. Lima, T. P. Segato, I. Cesarino, J. L. M. Cetino, S. A. S. Machado, F. Gomez, E. Carrilho, *Lab Chip* **2012**, *12*, 1959.
- [132] L. Ge, P. Wang, S. Ge, N. Li, J. Yu, M. Yan, J. Huang, *Anal. Chem.* **2013**, *85*, 3961.
- [133] X. Li, Z. Chen, Y. Zhong, F. Yang, J. Pan, Y. Liang, *Anal. Chim. Acta* **2012**, *710*, 118.
- [134] R. Malhotra, V. Patel, J. P. Vaqué, J. S. Gutkind, J. F. Rusling, *Anal. Chem.* **2010**, *82*, 3118.
- [135] X. Yu, B. Munge, V. Patel, G. Jensen, A. Bhirde, J. D. Gong, S. N. Kim, J. Gillespie, J. S. Gutkind, F. Papadimitrakopoulos, J. F. Rusling, *J. Am. Chem. Soc.* **2006**, *34*, 11199.
- [136] O. Bakajin, N. Ben-barak, J. Peng, A. Noy, presented at 7th Int. Conf. on Miniaturized Chemical and Biochemical Analysts Systems, Squaw Valley, CA USA, October 2003.
- [137] R. García-Fandiño, M. S. P. Sansom, *Proc. Natl. Acad. Sci. USA* **2012**, *109*, 6939.
- [138] K. Donaldson, C. A. Poland, F. A. Murphy, M. MacFarlane, T. Chernova, A. Schinwald, *Adv. Drug Delivery Rev.* **2013**, *65*, 2078.
- [139] C. P. Firme3rd, P. R. Bandaru, *Nanomedicine* **2010**, *6*, 245.
- [140] C. A. Poland, R. Duffin, I. Kinloch, A. Maynard, W. A. H. Wallace, A. Seaton, V. Stone, S. Brown, W. Macnee, K. Donaldson, *Nat. Nanotechnol.* **2008**, *3*, 423.
- [141] E. Heister, C. Lamprecht, V. Neves, C. Tilmaciu, L. Datas, E. Flahaut, B. Soula, P. Hinterdorfer, H. M. Coley, S. R. P. Silva, J. McFadden, *ACS Nano* **2010**, *4*, 2615.
- [142] K. Bhattacharya, S. P. Mukherjee, A. Gallud, S. C. Burkert, S. Bistarelli, S. Bellucci, M. Bottini, A. Star, B. Fadeel, *Nanomedicine* **2016**, *12*, 333.
- [143] X. M. Li, L. Wang, Y. B. Fan, Q. L. Feng, F. Z. Qui, *J. Nanomater.* **2012**, *2012*, 548389.
- [144] G. A. Akçeoğlu, O. L. Li, N. Saito, *Colloids Surf., B* **2015**, *136*, 1.
- [145] S. Yuyan, W. Jun, W. Hong, L. Jun, I. A. Aksay, L. Yuehe, *Electroanalysis* **2010**, *22*, 1027.
- [146] W.-W. Liu, S.-P. Chai, A. R. Mohamed, U. Hashim, *J. Ind. Eng. Chem.* **2014**, *20*, 1171.
- [147] J. R. Lomeda, C. D. Doyle, D. V. Kosynkin, W.-F. Hwang, J. M. Tour, *J. Am. Chem. Soc.* **2008**, *130*, 16201.
- [148] X. Zhong, J. Jin, S. Li, Z. Niu, W. Hu, R. Li, J. Ma, *Chem. Commun.* **2010**, *46*, 7340.
- [149] B. Konkena, S. Vasudevan, *Langmuir* **2012**, *28*, 12432.
- [150] Y. Song, Y. Luo, C. Zhu, H. Li, D. Du, Y. Lin, *Biosens. Bioelectron.* **2016**, *76*, 195.
- [151] L.-M. Lu, X.-L. Qiu, X.-B. Zhang, G.-L. Shen, W. Tan, R.-Q. Yu, *Biosens. Bioelectron.* **2013**, *45*, 102.
- [152] V. Mani, B. Devadas, S.-M. Chen, *Biosens. Bioelectron.* **2013**, *41*, 309.
- [153] K.-J. Huang, D.-J. Niu, J.-Y. Sun, C.-H. Han, Z.-W. Wu, Y.-L. Li, X.-Q. Xiong, *Colloids Surf., B* **2011**, *82*, 543.
- [154] N. M. Mubarak, E. C. Abdullah, N. S. Jayakumar, J. N. Sahu, *J. Ind. Eng. Chem.* **2014**, *20*, 1186.
- [155] A. K. Yagati, J. Park, S. Cho, *Sensors* **2016**, *16*, 109.
- [156] W. He, Y. Sun, J. Xi, A. A. M. Abdurhman, J. Ren, H. Duan, *Anal. Chim. Acta* **2016**, *903*, 61.
- [157] T. Feng, X. Qiao, H. Wang, Z. Sun, Y. Qi, C. Hong, *J. Mater. Chem. B* **2016**, *4*, 990.
- [158] W. Asghar, H. Shafiee, V. Velasco, V. R. Sah, S. Guo, R. El Assal, F. Inci, A. Rajagopalan, M. Jahangir, R. M. Anchan, G. L. Mutter, M. Ozkan, C. S. Ozkan, U. Demirci, *Sci. Rep.* **2016**, *6*, 30270.
- [159] P. S. Kumar, S. Priti, S. Jyoti, S. Sadhana, S. Sameer, S. S. Kumar, *Electroanalysis* **2016**, *28*, 2472.
- [160] D. Zhang, Q. Liu, *Biosens. Bioelectron.* **2016**, *75*, 273.
- [161] J. Li, J. Wu, L. Cui, M. Liu, F. Yan, H. Ju, *Analyst* **2016**, *141*, 131.
- [162] F.-Y. Kong, S.-X. Gu, W.-W. Li, T.-T. Chen, Q. Xu, W. Wang, *Biosens. Bioelectron.* **2014**, *56*, 77.
- [163] E. T. S. G. da Silva, D. E. P. Souto, J. T. C. Barragan, J. de F. Giarola, A. C. M. de Moraes, L. T. Kubota, *ChemElectroChem* **2017**, *4*, 778.
- [164] J. Rodriguez, G. Castaneda, I. Lizcano, *Electrochim. Acta* **2018**, *269*, 668.
- [165] M. Cadkova, A. Kovarova, V. Dvorakova, R. Metelka, Z. Bilkova, L. Korecka, *Talanta* **2018**, *182*, 111.
- [166] M. Hatada, W. Tsugawa, E. Kamio, N. Loew, D. C. Klonoff, K. Sode, *Biosens. Bioelectron.* **2017**, *88*, 167.
- [167] P. T. Garcia, L. N. Guimaraes, A. A. Dias, C. J. Ulhoa, W. K. T. Coltro, *Sens. Actuators, B* **2018**, *258*, 342.
- [168] D. Rodrigo, O. Limaj, D. Janner, D. Etezadi, F. J. Garcia De Abajo, V. Pruneri, H. Altug, *Science* **2015**, *349*, 165.
- [169] K. Chen, X. Zhou, X. Cheng, R. Qiao, Y. Cheng, C. Liu, Y. Xie, W. Yu, F. Yao, Z. Sun, F. Wang, K. Liu, Z. Liu, *Nat. Photonics* **2019**, *13*, 754.
- [170] E. O. Polat, G. Mercier, I. Nikitskiy, E. Puma, T. Galan, S. Gupta, M. Montagut, J. J. Piqueras, M. Bouwens, T. Durduran, G. Konstantatos, S. Goossens, F. Koppens, *Sci. Adv.* **2019**, *5*, eaaw7846.
- [171] Y. Qiao, X. Li, T. Hirtz, G. Deng, Y. Wei, M. Li, S. Ji, Q. Wu, J. Jian, F. Wu, Y. Shen, H. Tian, Y. Yang, T. L. Ren, *Nanoscale* **2019**, *11*, 18923.
- [172] A. V. Nielsen, M. J. Beauchamp, G. P. Nordin, A. T. Woolley, *Annu. Rev. Anal. Chem.* **2020**, *13*, 45.
- [173] S. Tasoglu, A. Folch, *Micromachines* **2018**, *9*, 609.
- [174] G. K. Monia Kabandana, C. G. Jones, S. K. Sharifi, C. Chen, *ACS Sens.* **2020**, *5*, 2044.
- [175] M. J. Beauchamp, G. P. Nordin, A. T. Woolley, *Anal. Bioanal. Chem.* **2017**, *409*, 4311.
- [176] G. Weisgrab, A. Ovsianikov, P. F. Costa, *Adv. Mater. Technol.* **2019**, *4*, 1900275.
- [177] F. P. W. Melchels, J. Feijen, D. W. Grijpma, *Biomaterials* **2010**, *31*, 6121.
- [178] M. Farsari, *2016 Conf. Lasers Electro-Optics, CLEO 2016*, Optical Society of America, Rochester NY **2016**.
- [179] J. R. Tumbleston, D. Shirvanyants, N. Ermoshkin, R. Januszewicz, A. R. Johnson, D. Kelly, K. Chen, R. Pinschmidt, J. P. Rolland, A. Ermoshkin, E. T. Samulski, J. M. DeSimone, *Science* **2015**, *347*, 1349.
- [180] M. P. De Beer, H. L. Van Der Laan, M. A. Cole, R. J. Whelan, M. A. Burns, T. F. Scott, *Sci. Adv.* **2019**, *5*, eaau8723.
- [181] B. E. Kelly, I. Bhattacharya, H. Heidari, M. Shusteff, C. M. Spadaccini, H. K. Taylor, *Science* **2019**, *363*, 1075.
- [182] A. Waldbaur, H. Rapp, K. Länge, B. E. Rapp, *Anal. Methods* **2011**, *3*, 2681.
- [183] R. D. Sochol, E. Sweet, C. C. Glick, S. Venkatesh, A. Avetisyan, K. F. Ekman, A. Raulinaitis, A. Tsai, A. Wienkers, K. Korner, K. Hanson, A. Long, B. J. Hightower, G. Slatton, D. C. Burnett,

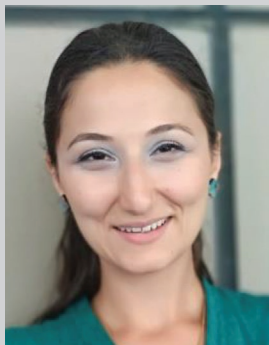
- T. L. Massey, K. Iwai, L. P. Lee, K. S. J. Pister, L. Lin, *Lab Chip* **2016**, *16*, 668.
- [184] N. P. Macdonald, J. M. Cabot, P. Smejkal, R. M. Guijt, B. Paull, M. C. Breadmore, *Anal. Chem.* **2017**, *89*, 3858.
- [185] X. Kuang, K. Chen, C. K. Dunn, J. Wu, V. C. F. Li, H. J. Qi, *ACS Appl. Mater. Interfaces* **2018**, *10*, 7381.
- [186] G. I. J. Salentijn, P. E. Oomen, M. Grajewski, E. Verpoorte, *Anal. Chem.* **2017**, *13*, 7053.
- [187] V. Romanov, R. Samuel, M. Chaharlang, A. R. Jafek, A. Frost, B. K. Gale, *Anal. Chem.* **2018**, *90*, 10450.
- [188] J. Loessberg-Zahl, A. D. Van der Meer, A. Van Den Berg, J. C. T. Eijkel, *Lab Chip* **2019**, *19*, 206.
- [189] S. Oh, B. Kim, J. K. Lee, S. Choi, *Sens. Actuators, B* **2018**, *259*, 106.
- [190] Y. S. Lee, N. Bhattacharjee, A. Folch, *Lab Chip* **2018**, *18*, 1207.
- [191] H. N. Chan, Y. Shu, B. Xiong, Y. Chen, Y. Chen, Q. Tian, S. A. Michael, B. Shen, H. Wu, *ACS Sens.* **2016**, *1*, 227.
- [192] S. Begolo, D. V. Zhukov, D. A. Selck, L. Li, R. F. Ismagilov, *Lab Chip* **2014**, *14*, 4616.
- [193] A. Kalantarifard, E. Alizadeh-Haghighi, A. Saateh, C. Elbuken, *Chem. Eng. Sci.* **2021**, *229*, 116093.
- [194] T. Glawdel, C. Elbuken, C. L. Ren, *Encyclopedia of Microfluidics and Nanofluidics*, Springer, Berlin **2013**.
- [195] S. Knowlton, C. H. Yu, F. Ersoy, S. Emadi, A. Khademhosseini, S. Tasoglu, *Biofabrication* **2016**, *8*, 025019.
- [196] I. Khan, A. Prabhakar, C. Delepine, H. Tsang, V. Pham, M. Sur, *Biomicrofluidics* **2021**, *15*, 024105.
- [197] R. W. Yucha, K. S. Hobbs, E. Hanhauser, L. E. Hogan, W. Nieves, M. O. Ozen, F. Inci, V. York, E. A. Gibson, C. Thanh, H. Shafiee, R. El Assal, M. Kiselinova, Y. P. Robles, H. Bae, K. S. Leadabrand, S. Q. Wang, S. G. Deeks, D. R. Kuritzkes, U. Demirci, T. J. Henrich, *EBioMedicine* **2017**, *20*, 217.
- [198] Q. Xu, M. Hashimoto, T. T. Dang, T. Hoare, D. S. Kohane, G. M. Whitesides, R. Langer, D. G. Anderson, H. David, *Small* **2009**, *5*, 1575.
- [199] J. Wan, *Polymers* **2012**, *4*.
- [200] B. Amoyav, Y. Goldstein, E. Steinberg, O. Benny, *Pharmaceutics* **2021**, *13*, 13.
- [201] K. Alessandri, M. Feyeux, B. Gurchenkov, C. Delgado, A. Trushko, K. H. Krause, D. Vignjević, P. Nassoy, A. Roux, *Lab Chip* **2016**, *16*, 1593.
- [202] C. Chen, B. T. Mehl, A. S. Munshi, A. D. Townsend, D. M. Spence, R. S. Martin, *Anal. Methods* **2016**, *8*, 6005.
- [203] S. Waheed, J. M. Cabot, N. P. Macdonald, T. Lewis, R. M. Guijt, B. Paull, M. C. Breadmore, *Lab Chip* **2016**, *16*, 1993.
- [204] F. A. Gomez, *Bioanalysis* **2013**, *5*, 1.
- [205] U. H. Yildiz, F. Inci, S. Wang, M. Toy, H. C. Tekin, A. Javaid, D. T.-Y. Lau, U. Demirci, *Biotechnol. Adv.* **2015**, *33*, 178.
- [206] H. Shafiee, E. A. Lidstone, M. Jahangir, F. Inci, E. Hanhauser, T. J. Henrich, D. R. Kuritzkes, B. T. Cunningham, U. Demirci, *Sci. Rep.* **2014**, *4*, 1.
- [207] F. Inci, M. G. Karaaslan, A. Mataji-Kojouri, P. A. Shah, Y. Saylan, Y. Zeng, A. Avadhani, R. Sinclair, D. T. Y. Lau, U. Demirci, *Appl. Mater. Today* **2020**, *20*, 100709.
- [208] M. Li, T. Chen, J. J. Gooding, J. Liu, *ACS Sens.* **2019**, *4*, 1732.
- [209] O. Tokel, F. Inci, U. Demirci, *Chem. Rev.* **2014**, *114*, 5728.
- [210] Y. Saylan, Ö. Erdem, N. Cihangir, A. Denizli, *Chemosensors* **2019**, *7*, 33.
- [211] E. Petryayeva, U. J. Krull, *Anal. Chim. Acta* **2011**, *706*, 8.
- [212] S. Akhavan, M. Z. Akgul, P. L. Hernandez-Martinez, H. V. Demir, *ACS Nano* **2017**, *11*, 5430.
- [213] F. Inci, Y. Saylan, A. M. Kojouri, M. G. Ogut, A. Denizli, U. Demirci, *Appl. Mater. Today* **2020**, *18*, 100478.
- [214] R. Ahmed, M. O. Ozen, M. G. Karaaslan, C. A. Prator, C. Thanh, S. Kumar, L. Torres, N. Iyer, S. Munter, S. Southern, T. J. Henrich, F. Inci, U. Demirci, *Adv. Mater.* **2020**, *32*, 1907160.
- [215] M. Rycenga, C. M. Cobley, J. Zeng, W. Li, C. H. Moran, Q. Zhang, D. Qin, Y. Xia, *Chem. Rev.* **2011**, *111*, 3669.
- [216] Ö. Erdem, Y. Saylan, N. Cihangir, A. Denizli, *Biosens. Bioelectron.* **2019**, *126*, 608.
- [217] S. Unser, I. Bruzas, J. He, L. Sagle, *Sensors* **2015**, *15*, 15684.
- [218] Z. Li, L. Leustean, F. Inci, M. Zheng, U. Demirci, S. Wang, *Biotechnol. Adv.* **2019**, *37*, 107440.
- [219] R. Funari, K. Y. Chu, A. Q. Shen, *Biosens. Bioelectron.* **2020**, *169*, 112578.
- [220] R. de la Rica, M. M. Stevens, *Nat. Nanotechnol.* **2012**, *7*, 821.
- [221] H. Shafiee, W. Asghar, F. Inci, M. Yuksekkaya, M. Jahangir, M. H. Zhang, N. G. Durmus, U. A. Gurkan, D. R. Kuritzkes, U. Demirci, *Sci. Rep.* **2015**, *5*, 8719.
- [222] P. Moitra, M. Alafeef, M. Alafeef, M. Alafeef, K. Dighe, M. B. Frieman, D. Pan, D. Pan, D. Pan, *ACS Nano* **2020**, *14*, 7617.
- [223] J. L. Arlett, E. B. Myers, M. L. Roukes, *Nat. Nanotechnol.* **2011**, *6*, 203.
- [224] T. Braun, M. K. Ghatkesar, N. Backmann, W. Grange, P. Boulanger, L. Letellier, H.-P. Lang, A. Bietsch, C. Gerber, M. Hegner, *Nat. Nanotechnol.* **2009**, *4*, 179.
- [225] N. Backmann, C. Zahnd, F. Huber, A. Bietsch, A. Plückthun, H.-P. Lang, H.-J. Güntherodt, M. Hegner, C. Gerber, *Proc. Natl. Acad. Sci. USA* **2005**, *102*, 14587.
- [226] J. Mertens, C. Rogero, M. Calleja, D. Ramos, J. A. Martín-Gago, C. Briones, J. Tamayo, *Nat. Nanotechnol.* **2008**, *3*, 301.
- [227] T. Braun, N. Backmann, M. Vögli, A. Bietsch, A. Engel, H.-P. Lang, C. Gerber, M. Hegner, *Biophys. J.* **2006**, *90*, 2970.
- [228] C. Lissandrello, F. Inci, M. Francom, M. R. Paul, U. Demirci, K. L. Ekin, *Appl. Phys. Lett.* **2014**, *105*, 113701.
- [229] M. Gürgöze, H. Erol, *J. Sound Vib.* **2006**, *298*, 132.
- [230] L. Mazutis, J. Gilbert, W. L. Ung, D. A. Weitz, A. D. Griffiths, J. A. Heyman, *Nat. Protoc.* **2013**, *8*, 870.
- [231] H. Etayash, M. F. Khan, K. Kaur, T. Thundat, *Nat. Commun.* **2016**, *7*, 12947.
- [232] S. Akgönüllü, D. Battal, M. S. Yalcin, H. Yavuz, A. Denizli, *Micro. J.* **2020**, *153*, 104454.
- [233] F. Inci, *Lipid Bilayers and Liposomes on Microfluidics Realm: Techniques and Applications*, Springer Nature Switzerland, Switzerland **2019**, pp. 213–223.
- [234] N. J. Ronkainen, H. B. Halsall, W. R. Heineman, *Chem. Soc. Rev.* **2010**, *39*, 1747.
- [235] D. Grieshaber, R. MacKenzie, J. Vörös, E. Reimhult, *Sensors* **2008**, *8*, 1400.
- [236] J. Tan, J. Xu, *Artif. Intell. Agric.* **2020**, *4*, 104.
- [237] K. R. Rogers, *Mol. Biotechnol.* **2000**, *14*, 109.
- [238] P. He, Y. Xu, Y. Fang, *Anal. Lett.* **2005**, *38*, 2597.
- [239] L. Wu, H. Ji, Y. Guan, X. Ran, J. Ren, X. Qu, *NPG Asia Mater.* **2017**, *9*, e356.
- [240] M. Yucel, O. Akin, M. Cayoren, I. Akduman, A. Palaniappan, B. Liedberg, G. Hizal, F. Inci, U. H. Yildiz, *Anal. Chem.* **2018**, *90*, 5122.
- [241] G. Xu, J. Abbott, L. Qin, K. Y. M. Yeung, Y. Song, H. Yoon, J. Kong, D. Ham, *Nat. Commun.* **2014**, *5*, 4866.
- [242] S. Islam, S. Shukla, V. K. Bajpai, Y. K. Han, Y. S. Huh, A. Ghosh, S. Gandhi, *Sci. Rep.* **2019**, *9*, 276.
- [243] H. Shafiee, M. Jahangir, F. Inci, S. Wang, R. B. M. Willenbrecht, F. F. Giguel, A. M. N. Tsibris, D. R. Kuritzkes, U. Demirci, *Small* **2013**, *9*, 2553.
- [244] V. Gubala, L. F. Harris, A. J. Ricco, M. X. Tan, D. E. Williams, *Anal. Chem.* **2012**, *84*, 487.
- [245] Y. Saylan, A. Denizli, *Micromachines* **2019**, *10*, 766.
- [246] Y. Song, Y.-Y. Huang, X. Liu, X. Zhang, M. Ferrari, L. Qin, *Trends Biotechnol.* **2014**, *32*, 132.
- [247] W. Jung, J. Han, J.-W. Choi, C. H. Ahn, *Microelectron. Eng.* **2015**, *132*, 46.

- [248] B. V. Chikkaveeraiah, V. Mani, V. Patel, J. S. Gutkind, J. F. Rusling, *Biosens. Bioelectron.* **2011**, *26*, 4477.
- [249] N. P. Sardesai, K. Kadimisetty, R. Faria, J. F. Rusling, *Anal. Bioanal. Chem.* **2013**, *405*, 3831.
- [250] R. Malhotra, V. Patel, B. V. Chikkaveeraiah, B. S. Munge, S. C. Cheong, R. B. Zain, M. T. Abraham, D. K. Dey, J. S. Gutkind, J. F. Rusling, *Anal. Chem.* **2012**, *84*, 6249.
- [251] B. H. Shadfan, A. R. Simmons, G. W. Simmons, A. Ho, J. Wong, K. H. Lu, R. C. J. Bast, J. T. McDevitt, *Cancer Prev. Res.* **2015**, *8*, 37.
- [252] J. Mok, M. N. Mindrinos, R. W. Davis, M. Javanmard, *Proc. Natl. Acad. Sci. USA* **2014**, *111*, 2110 LP.
- [253] A. D. Warren, G. A. Kwong, D. K. Wood, K. Y. Lin, S. N. Bhatia, *Proc. Natl. Acad. Sci. USA* **2014**, *111*, 3671 LP.
- [254] X. Wei, T. Tian, S. Jia, Z. Zhu, Y. Ma, J. Sun, Z. Lin, C. J. Yang, *Anal. Chem.* **2016**, *88*, 2345.
- [255] I. K. Dimov, L. Basabe-Desmonts, J. L. Garcia-Cordero, B. M. Ross, A. J. Ricco, L. P. Lee, *Lab Chip* **2011**, *11*, 845.
- [256] Y. Song, Y. Zhang, P. E. Bernard, J. M. Reuben, N. T. Ueno, R. B. Arlinghaus, Y. Zu, L. Qin, *Nat. Commun.* **2012**, *3*, 1283.
- [257] C. D. Chin, T. Laksanasopin, Y. K. Cheung, D. Steinmiller, V. Linder, H. Parsa, J. Wang, H. Moore, R. Rouse, G. Umviligijozo, E. Karita, L. Mwambarangwe, S. L. Braunstein, J. Van De Wijgert, R. Sahabo, J. E. Justman, W. El-Sadr, S. K. Sia, *Nat. Med.* **2011**, *17*, 1015.
- [258] V. Nisenblatt, P. M. M. Bossuyt, R. Shaikh, C. Farquhar, V. Jordan, C. S. Scheffers, B. W. J. Mol, N. Johnson, M. L. Hull, *Cochrane Database Syst. Rev.* **2016**, *2016*, CD012179.
- [259] A. Jedinak, K. R. Loughlin, M. A. Moses, *Oncotarget* **2018**, *9*, 32534.
- [260] P. H. Lin, B. R. Li, *Analyst* **2020**, *145*, 1110.
- [261] A. Niemi, T. M. Ferguson, D. S. Boyle, *Trends Biotechnol.* **2011**, *29*, 240.
- [262] Cyclops, *Can. J. Ophthalmol.* **2013**, *48*, 349.
- [263] M. Liong, A. N. Hoang, J. Chung, N. Gural, C. B. Ford, C. Min, R. R. Shah, R. Ahmad, M. Fernandez-Suarez, S. M. Fortune, M. Toner, H. Lee, R. Weissleder, *Nat. Commun.* **2013**, *4*, 1752.
- [264] B. E. Root, A. K. Agarwal, D. M. Kelso, A. E. Barron, *Anal. Chem.* **2011**, *83*, 982.
- [265] X. Fang, Y. Liu, J. Kong, X. Jiang, *Anal. Chem.* **2010**, *82*, 3002.
- [266] S. Lutz, P. Weber, M. Focke, B. Faltin, J. Hoffmann, C. Müller, D. Mark, G. Roth, P. Munday, N. Armes, O. Piepenburg, R. Zengerle, F. von Stetten, *Lab Chip* **2010**, *10*, 887.
- [267] W.-H. Chang, S.-Y. Yang, C.-H. Wang, M.-A. Tsai, P.-C. Wang, T.-Y. Chen, S.-C. Chen, G.-B. Lee, *Sens. Actuators, B* **2013**, *180*, 96.
- [268] X. Lin, X. Huang, K. Urmann, X. Xie, M. R. Hoffmann, *ACS Sens.* **2019**, *4*, 242.
- [269] X. Jiang, W. Jing, X. Sun, Q. Liu, C. Yang, S. Liu, K. Qin, G. Sui, *ACS Sens.* **2016**, *1*, 958.
- [270] F. Inci, U. Celik, B. Turken, H. Ö. Özer, F. N. Kok, *Biochem. Biophys. Rep.* **2015**, *2*, 115.
- [271] A. Halperin, A. Buhot, E. B. Zhulina, *Langmuir* **2006**, *22*, 11290.
- [272] P. M. Arnott, H. Joshi, A. Aksimentiev, S. Howorka, *Langmuir* **2018**, *34*, 15084.
- [273] H. M. Tay, R. Dalan, K. H. H. Li, B. O. Boehm, H. W. Hou, *Small* **2018**, *14*, 1702832.
- [274] M. Hoyos-Nogués, S. Brosel-Oliu, N. Abramova, F. X. Muñoz, A. Bratov, C. Mas-Moruno, F. J. Gil, *Biosens. Bioelectron.* **2016**, *86*, 377.
- [275] X. Yu, Y. Xia, Y. Tang, W. L. Zhang, Y. T. Yeh, H. Lu, S. Y. Zheng, *Small* **2017**, *13*, 1700425.
- [276] A. M. Foudeh, T. Fatanat Didar, T. Veres, M. Tabrizian, *Lab Chip* **2012**, *12*, 3249.
- [277] P. Yager, T. Edwards, E. Fu, K. Helton, K. Nelson, M. R. Tam, B. H. Weigl, *Nature* **2006**, *442*, 412.
- [278] B. Weigl, G. Domingo, P. Labarre, J. Gerlach, *Lab Chip* **2008**, *8*, 1999.
- [279] S. Marre, K. F. Jensen, *Chem. Soc. Rev.* **2010**, *39*, 1183.
- [280] R. G. Blazej, P. Kumaresan, R. A. Mathies, *Proc. Natl. Acad. Sci. USA* **2006**, *103*, 7240.
- [281] D. T. Chiu, R. M. Lorenz, *Acc. Chem. Res.* **2009**, *42*, 649.
- [282] E. Gencturk, S. Mutlu, K. O. Ulgen, *Biomicrofluidics* **2017**, *11*, 051502.
- [283] S. Chisca, P. H. H. Duong, A. H. Emwas, R. Sougrat, S. P. Nunes, *Polym. Chem.* **2015**, *6*, 543.
- [284] J. C. McDonald, S. J. Metallo, G. M. Whitesides, *Anal. Chem.* **2001**, *73*, 5645.
- [285] A. Polini, E. Mele, A. G. Sciancalepore, S. Girardo, A. Biasco, A. Camposeo, R. Cingolani, D. A. Weitz, D. Pisignano, *Biomicrofluidics* **2010**, *4*, 036502.
- [286] S. Akay, R. Heils, H. K. Trieu, I. Smirnova, O. Yesil-Celiktas, *Carbohydr. Polym.* **2017**, *161*, 228.
- [287] K. Kim, S. W. Park, S. S. Yang, *BioChip J.* **2010**, *4*, 148.
- [288] S. Nishat, A. T. Jafry, A. W. Martinez, F. R. Awan, *Sens. Actuators, B* **2021**, *336*, 129681.
- [289] A. W. Martinez, S. T. Phillips, E. Carrilho, S. W. Thomas, H. Sindi, G. M. Whitesides, *Anal. Chem.* **2008**, *80*, 3699.
- [290] K. A. Ganaja, C. A. Chaplan, J. Zhang, N. W. Martinez, A. W. Martinez, *Anal. Chem.* **2017**, *89*, 5333.
- [291] A. W. Martinez, S. T. Phillips, G. M. Whitesides, *Proc. Natl. Acad. Sci. USA* **2008**, *105*, 19606.
- [292] D. Wei, Y. Liu, *Adv. Mater.* **2010**, *22*, 3225.
- [293] E. M. Materón, R. S. Lima, N. Joshi, F. M. Shimizu, O. N. Oliveira, *Graphene-Based Electrochemical Sensors for Biomolecules*, Elsevier, Amsterdam **2018**, pp. 321–326.
- [294] R. Singh, D. Pantarotto, D. McCarthy, O. Chaloin, J. Hoebeke, C. D. Partidos, J. P. Briand, M. Prato, A. Bianco, K. Kostarelos, *J. Am. Chem. Soc.* **2005**, *127*, 4388.
- [295] P. Ravichandran, S. Baluchamy, R. Gopikrishnan, S. Biradar, V. Ramesh, V. Goornavar, R. Thomas, B. L. Wilson, R. Jeffers, J. C. Hall, G. T. Ramesh, *J. Biol. Chem.* **2011**, *286*, 29725.
- [296] N. L. Guo, Y. W. Wan, J. Denvir, D. W. Porter, M. Pacurari, M. G. Wolfarth, V. Castranova, Y. Qian, *J. Toxicol. Environ. Health, Part A* **2012**, *75*, 1129.
- [297] C. A. Poland, R. Duffin, I. Kinloch, A. Maynard, W. A. H. Wallace, A. Seaton, V. Stone, S. Brown, W. MacNee, K. Donaldson, *Nat. Nanotechnol.* **2008**, *3*, 423.
- [298] S. Shrivastava, T. Q. Trung, N. E. Lee, *Chem. Soc. Rev.* **2020**, *49*, 1812.
- [299] S. Q. Wang, D. Sarenac, M. H. Chen, S. H. Huang, F. F. Giguél, D. R. Kuritzkes, U. Demirci, *Int. J. Nanomed.* **2012**, *7*, 5019.
- [300] J. Kim, E. C. Jensen, A. M. Stockton, R. A. Mathies, *Anal. Chem.* **2013**, *85*, 7682.
- [301] M. W. L. Watson, M. J. Jebrail, A. R. Wheeler, *Anal. Chem.* **2010**, *82*, 6680.
- [302] E. A. Wagar, B. Yasin, S. Yuan, *Lab. Med.* **2008**, *39*, 560.
- [303] K. L. Hess, D. G. Fisher, G. L. Reynolds, *PLoS One* **2014**, *9*, e112190.
- [304] B. S. Karon, R. Scott, M. F. Burritt, P. J. Santrach, *Am. J. Clin. Pathol.* **2007**, *128*, 168.
- [305] J. L. Bock, A. J. Singer, H. C. Thode, *Am. J. Clin. Pathol.* **2008**, *130*, 132.
- [306] Y. Saylan, Ö. Erdem, F. Inci, A. Denizli, *Biomimetics* **2020**, *5*, 20.
- [307] M. Rasmussen, S. Abdellaoui, S. D. Minteer, *Biosens. Bioelectron.* **2016**, *76*, 91.
- [308] Z. L. Wang, W. Wu, *Angew. Chem., Int. Ed.* **2012**, *51*, 11700.
- [309] J. Su, V. Leonov, M. Goedbloed, Y. Van Andel, M. C. De Nooijer, R. Elfrink, Z. Wang, R. J. M. Vullers, *J. Micromech. Microeng.* **2010**, *20*, 104005.
- [310] M. M. Müller, W. Hackl, A. Griesmacher, *Anaesthesist* **1999**, *48*, 3.
- [311] D. C. Christodouleas, B. Kaur, P. Chorti, *ACS Cent. Sci.* **2018**, *4*, 1600.
- [312] T. Chinnasamy, J. L. Kingsley, F. Inci, P. J. Turek, M. P. Rosen, B. Behr, E. Tüzel, U. Demirci, *Adv. Sci.* **2018**, *5*, 1700531.
- [313] S. Deshmukh, F. Inci, M. G. Karaaslan, M. G. Ogut, D. Duncan, L. Klevan, G. Duncan, U. Demirci, *Forensic Sci. Int.: Genet.* **2020**, *48*, 102313.

- [314] F. Inci, M. G. Karaaslan, R. Gupta, A. Avadhani, M. G. Ogut, E. E. Atila, G. Duncan, L. Klevan, U. Demirci, *Forensic Sci. Int.: Genet.* **2021**, *52*, 102451.
- [315] F. Inci, M. O. Ozen, Y. Saylan, M. Miansari, D. Cimen, R. Dhara, T. Chinnasamy, M. Yuksekkaya, C. Filippini, D. K. Kumar, S. Calamak, Y. Yesil, N. G. Durmus, G. Duncan, L. Klevan, U. Demirci, *Adv. Sci.* **2018**, *5*, 1800121.
- [316] R. Konwarh, P. Gupta, B. B. Mandal, *Biotechnol. Adv.* **2016**, *34*, 845.
- [317] P. Domachuk, K. Tsioris, F. G. Omenetto, D. L. Kaplan, *Adv. Mater.* **2010**, *22*, 249.
- [318] Y. Ling, J. Rubin, Y. Deng, C. Huang, U. Demirci, J. M. Karp, A. Khademhosseini, *Lab Chip* **2007**, *7*, 756.
- [319] A. Hasan, A. Paul, N. E. Vrana, X. Zhao, A. Memic, Y. S. Hwang, M. R. Dokmeci, A. Khademhosseini, *Biomaterials* **2014**, *35*, 7308.
- [320] M. T. Sebastian, *Dielectric Materials for Wireless Communication*, Elsevier, Amsterdam **2008**.
- [321] Q. Yang, Z. Zhang, W. Zhu, G. Wang, *ACS Omega* **2019**, *4*, 5165.
- [322] X. Xin, C. Xu, D. Zhang, Z. Liu, W. Ma, X. Qian, M. L. Chen, J. Du, H. M. Cheng, W. Ren, *ACS Appl. Mater. Interfaces* **2019**, *11*, 17629.
- [323] F. Yan, M. Zhang, J. Li, *Adv. Healthcare Mater.* **2014**, *3*, 313.
- [324] W. Chen, L. Yan, P. R. Bangal, *J. Phys. Chem. C* **2010**, *114*, 19885.



Garbis Atam Akceoglu is a researcher at Bilkent University – UNAM. Earlier, he worked as an assistant professor at Okan University, Department of Genetics and Bioengineering. He graduated from Istanbul University, Department of Biology in 2007. He then received his M.Sc. degree from Istanbul Technical University, Department of Molecular Biology Genetics and Biotechnology in 2011. Afterward, he completed his Ph.D. education at Nagoya University, Department of Physics, Energy, and Material Engineering in 2016. His research areas focus on bonding forces and bio-interface between carbonaceous materials and biological structures on various systems such as point-of-care diagnostic devices and microfluidic systems.



Yeşeren Saylan is currently working as an assistant professor at Hacettepe University, Department of Chemistry, Ankara, Turkey. She graduated from Hacettepe University, Department of Chemistry in 2008. She then received her M.Sc. and Ph.D. degrees from Hacettepe University, Department of Chemistry, Division of Biochemistry in 2011 and 2017, respectively. Earlier, she worked as a visiting researcher at Stanford University, School of Medicine, Palo Alto, CA, U.S.A. She is particularly dedicated to developing precise sensing platforms for medical diagnostics, environmental monitoring, food safety, as well as rationally designing specific molecularly imprinted polymeric materials at micro- and nanoscales for various applications.



Fatih Inci is an assistant professor at Bilkent University – UNAM. Earlier, he worked as an academician and postdoctoral researcher at Stanford University School of Medicine, Harvard Medical School-Brigham and Women's Hospital, and Harvard-MIT. His research focuses on the development of microfluidics and biosensors for medical diagnostics. He has published 50+ papers, 8 book chapters (3 chapters in-press) and 3 editorials; edited 3 books (2 books in-progress). He holds 8 patents (issued/submitted) and 2 licensed-products and his work has been highlighted by NIH–NIBIB, NIJ, Science–AAAS, Nature Medicine, AIP, JAMA, Newsweek, and Popular Science.